Supplementary Information for

Selenol-containing two-dimensional perovskite promotes visible-light-driven selective reduction of unsaturated ketones

Wenxuan Li,†[a] Lihao Liao,†[a] Guoying Yao,[ab] Jialong Liu,[a] Yilan Zhang,[a] Jingpeng Li,[a] Wangzhen Qiu,[a] Tao Zeng,*[b] Xiaodan Zhao*[a] and Zhenyu Yang*[a]

[a.]MOE Laboratory of Bioinorganic and Synthetic Chemistry, Lehn Institute of Functional Materials, School of Chemistry, Sun Yat-sen University, Guangzhou, Guangdong, China, 510275.

[b.]Department of Chemistry, York University, Toronto, ON, Canada, M3J 1P3.

†These authors contributed equally to this work.

Keywords: metal halide perovskites, two-dimensionality, selenol, photocatalysis, selective reduction

Corresponding author: tzeng@yorku.ca (T.Z.); zhaoxd3@mail.sysu.edu.cn (X.Z.); yangzhy63@mail.sysu.edu.cn (Z.Y.)

Table of Content

1. General information 3

2. Structural and optical properties study of TMHPs 6

3. Substrates synthesis 14

4. Summary of NMR data 19

5. Supplementary NMR spectra for products 28

6. Mechanism study 51

7. References 56

1. General information

Materials. 2,2'-diselanediyldie thanamine dihydrochloride ($DSEACl_2$, 97%) was purchased from Beijing Innochem Science & Technology Co., Ltd. Hydriodic acid (HI, 57% w/w), hypophosphorous acid (H_3PO_2, 50% w/w), and lead (II) iodide (PbI_2, 98%) were purchased from Aladdin Inc. Trichloromethane (99.0%) was purchased from Guangzhou Chemical Reagent Inc. Deuterated chloroform ($CDCl_3$, 99.8%) and deuterated dimethyl sulfoxide (DMSO-d_6, 99.8%) were purchased from Energy Chemical Inc. Petroleumether (PE, 99.7%), ethylacetate (EA, 99.5%) and *n*-hexane (97.0%) were purchased from Aladdin Inc. All chemicals were used as received without further purification. Detailed preparation approaches of all ketone substrates are available in Supplementary Information Section 2.

Preparation of $(SEA)_2PbI_4$ single crystal. 31.8 mg of $DSEACl_2$ (0.10 mmol) and 41.6 mg of PbI_2 (0.10 mmol) were transferred to a 10 mL thick-walled reaction tube and further dissolved in a mixed solution containing 0.50 mL of 57% w/w HI and 0.10 mL of 50% w/w H_3PO_2. The solution was heated to 110 °C with mechanical stirring until the solids were completely dissolved. Upon gradual natural cooling to room temperature, orange plate-like crystals gradually formed and precipitated. The product crystals were collected using Buchner filtration and finally transferred to a nitrogen-filled glovebox for storage.

Powder and single-crystal X-ray diffraction (PXRD and SXRD). PXRD patterns were recored on a Rigaku Miniflex 600 diffractometer (Cu-Kα, λ = 1.5406 Å) operating at a voltage of 45 kV and a current of 15 mA. SXRD data were collected using an Agilent SuperNova diffractometer with the nomochromatized Ga- Kα (λ=1.34138 Å) source at 150 K. The crystal structure was solved by direct methods and refined via full matrix least-square technique using SHELXL with OLEX2-1.5 package.

Stereo fluorescence microscope (SFM) imaging. The crystal sample was placed on a clean silicon wafer (2 cm × 2 cm) and imaged using a Leica M205FA stereomicroscope with visible light or 365 nm UV illumination.

Photoluminescence (PL) and absorption spectroscopy. The PL spectrum of the crystalline sample was recorded at 77 K using an FLS1000 spectrometer (Edinburgh Instruments) equipped with a xenon lamp and monochromator. The excitation wavelength of the PL spectrum was set at 370 nm. The absorption spectrum was recorded using a UV3600 fluorometer (Shimadzu Inc.).

Raman spectroscopy. The Raman spectrum was recorded using a TriVista 557 spectrometer (Princeton Instruments) with a 785 nm laser (power: 1 mW) as the excitation source.

Computational studies. All solid state quantum chemistry computations were done using the Vienna ab initio simulation package (VASP-5.4.4)[1] with the projector augmented-wave (PAW) potentials[2] and PBE functional[3]. The cut off energy for plane wave basis set was set to 400 eV. The k-points were set according to lattice parameters and summarized in Table S3. The LOBSTER-2.1.0 program was used to generate the DOS and pDOS[4]. All crystal structures were plotted using VESTA-3.5.5[5]. The reaction Gibbs free energies were obtained through molecular DFT calculations using ORCA with the def2-SVP basis set the wB97x functional, and the PCM solvent model with toluene as the solvent. Since all the elementary reactions occur in condensed phase, where molecular translation and rotation are (at least partially) hindered, we only include the vibrational contribution to the Gibbs free energy in evaluating the reaction Gibbs free energies.

NMR spectroscopy. ^{1}H, $^{19}F\{^{1}H\}$ and $^{13}C\{^{1}H\}$ NMR spectra were recorded on a Bruker Avance III 400 MHz spectrometer at ambient temperature. Samples (~5 mg) were dissolved in $CDCl_3$ or DMSO-d_6 and ultrasonicated for ~1 min to form homogenous dispersion. MestReNova software (ver.14.2.1, Mestrelab Research) was used to analyze the NMR results. All chemical shifts were recorded in parts per million (ppm, δ). ^{1}H NMR spectra are referred to the residual $CHCl_3$ signal (7.26 ppm) or residue DMSO signal (2.50 ppm), and ^{13}C NMR spectra are referred to the $CDCl_3$ signal (77.2 ppm, triplet) or DMSO-d_6 signal (39.6 ppm, septet). Data for ^{1}H NMR are reported as follows: chemical shift (δ ppm), multiplicity (s = singlet, d = doublet, t = triplet, q = quartet, m = multiplet), coupling constant (Hz), integration.

Data for $^{13}C\{^1H\}$ NMR, and $^{19}F\{^1H\}$ NMR are reported as follows: chemical shift (δ ppm), multiplicity (d = doublet, q = quartet), coupling constant (Hz). High resolution mass spectra of new compounds were recorded on LTQ Orbitrap Elite LC/MS (APCI).

Photocatalytic reduction of *α,β*-unsaturated ketones. A mixture of substrate **1** (0.1 mmol, 1 equiv), $(SEA)_2PbI_4$ (0.01 mmol, 0.1 equiv), and H_3PO_2 (1.2 mmol, 50 wt%) in *n*-hexane (2.0 mL) was transferred to a 10 mL glass vial. The vial was degassed with N_2, sealed, and placed onto the holder (5 cm above the light source (10 W, λ = 450 nm or 525 nm, PCX50B/50C, Beijing Perfectlight Technology Co., Ltd.)) for the photcatalytic reaction. The reaction lasted for a predesigned period with magnetic stirring at 60 ^oC. After that, the mixture was concentrated *in vacuo* and purified by preparative thin-layer chromatography to afford the reduction product **2.** Control experiments were conducted using the same conditions except for the specific description of the condition changes (e.g. absence of light, replacement of catalyst, or the addition of radical scavengers).

Hot filtration experiments. The photocatalytic reaction was first carried out under the standard conditions described above in the presence of $(SEA)_2PbI_4$. After 4 h of visible-light irradiation, the reaction reached approximately 20% conversion. At this point, the reaction mixture was quickly filtered at the reaction temperature to completely remove the solid photocatalyst. The obtained clear filtrate was then transferred to a clean glass vial and further irradiated under identical conditions for an additional 12 h. The reaction progress and product yields were determined by ^1H NMR spectroscopy using 1,3,5-trimethoxybenzene as the internal standard.

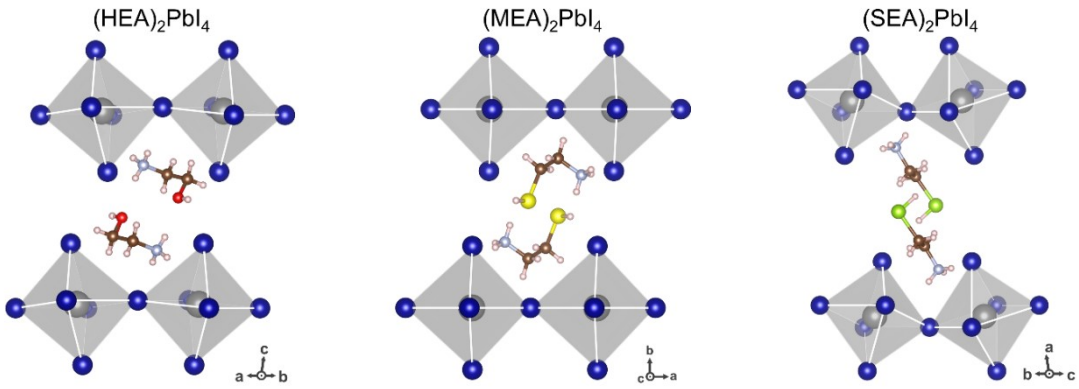

2. Structural and optical properties study of TMHPs

Figure S1. Single-crystal structures of $(HEA)_2PbI_4$, $(MEA)_2PbI_4$ and $(SEA)_2PbI_4$. (CCDC: $(HEA)_2PbI_4$[6]: 237189; $(MEA)_2PbI_4$[7]: 2059317; $(SEA)_2PbI_4$: 2348172)

Table S1. Summary of the elemental proportions near the valence band edge within the excitation ranges of blue (450 nm) and green light (525 nm) for the TMHPs containing chalcogenol functional groups (-OH, -SH, -SeH) as defined in Figure 1c.

Excitation	TMHP	Pb (%)	I (%)	C (%)	N (%)	O/S/Se (%)	H (%)
450 nm	$(HEA)PbI_4$	11.54	86.67	0.70	0.32	0.18	0.59
	$(MEA)_2PbI_4$	1.90	82.08	1.35	0.31	13.51	0.85
	$(SEA)_2PbI_4$	1.50	21.59	2.81	0.56	70.62	2.92
525 nm	$(MEA)_2PbI_4$	6.73	86.21	0.87	0.14	5.52	0.52
	$(SEA)_2PbI_4$	3.05	31.58	1.93	0.43	61.58	1.42

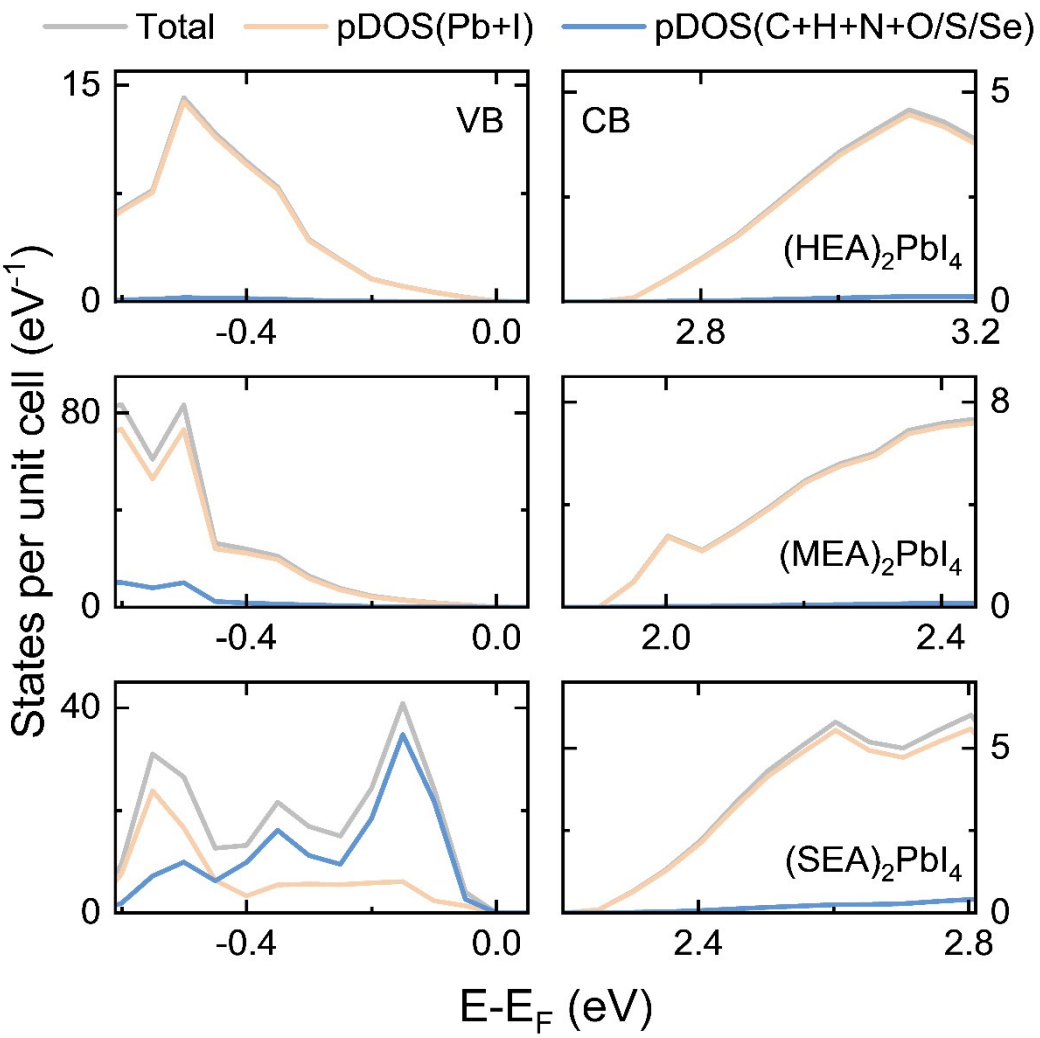

Figure S2. Zoom-in pDOS results for $(HEA)_2PbI_4$, $(MEA)_2PbI_4$, and $(SEA)_2PbI_4$ showing the organic and inorganic contributions near the band edges. The Fermi level is aligned at 0 eV.

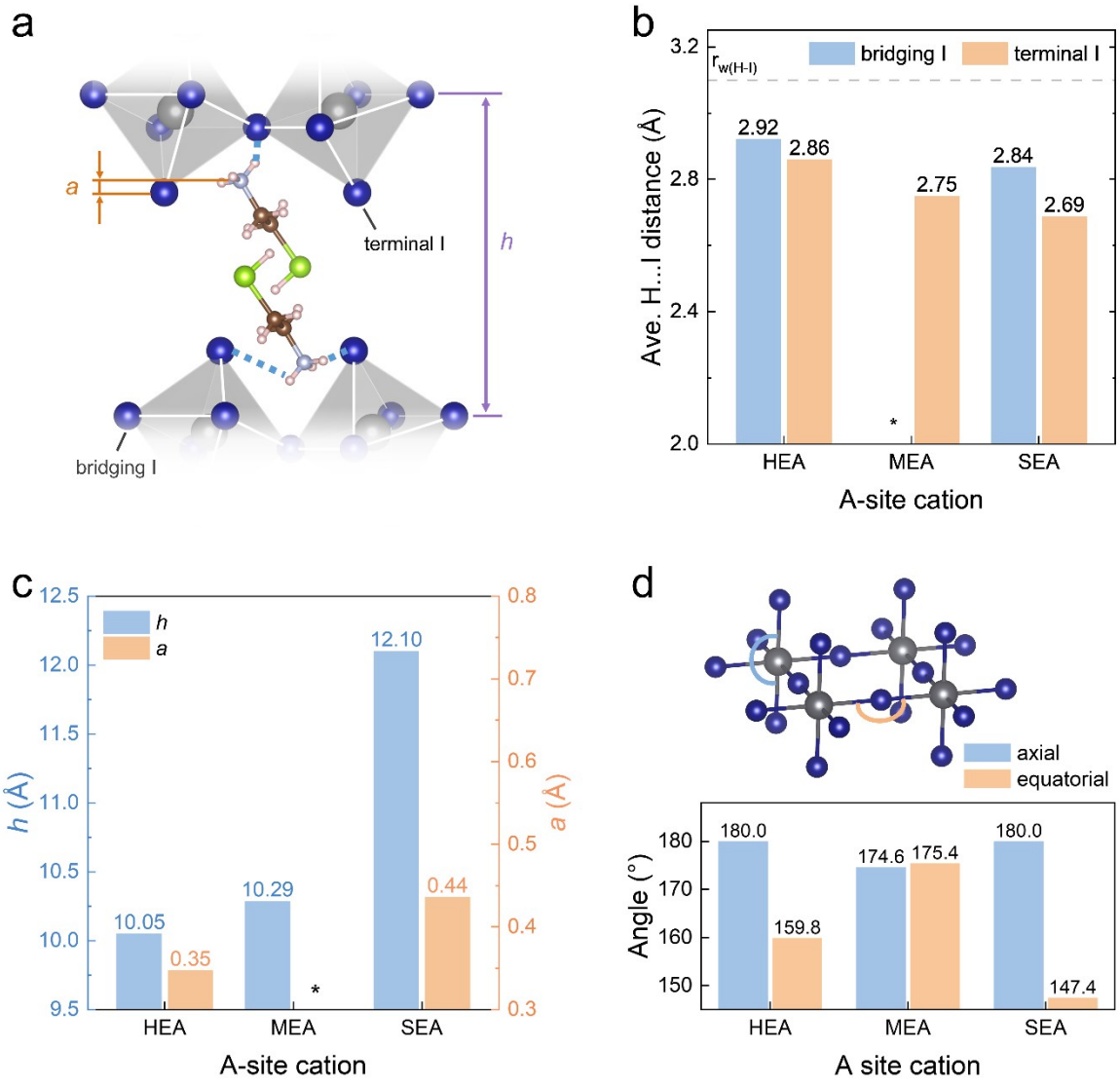

Figure S3. Structural analysis of $(HEA)_2PbI_4$, $(MEA)_2PbI_4$, and $(SEA)_2PbI_4$. (a) General crystal structure of TMHPs (taking $(SEA)_2PbI_4$ as the model), where *a* and *h* refer to the penetration depth of the cations and the distance between two adjacent planes for the Pb centers in the $[PbI_6]^{4-}$ octahedra, respectively. **(b)** H…I distance shown in (a). **(c)** Summary of the octahedral spacing values *h* and penetration depth *a* shown in (a). The asterisk denotes $a < 0$ for MEA-based structure. **(d)** Definition and summary of the axial I−Pb−I and the equatorial Pb−I−Pb angles.

Table S2. Data summary of TMHP single crystals studied in this work.

Compound	$(HEA)_2PbI_4$	$(MEA)_2PbI_4$	$(SEA)_2PbI_4$
Empirical Formula	$C_4H_{16}I_4N_2PbO_2$	$C_4H_{16}I_4N_2PbS_2$	$C_4H_{16}I_4N_2PbSe_2$
Crystal system	monoclinic	orthorhombic	monoclinic
Space group	*P21/a*	*Pnma*	*P21/a*
Color	orange	red	orange
Cell dimensions	a = 8.9350(10) Å	a = 12.9517(4) Å	a = 12.2377(6) Å
	b = 9.056(2) Å	b = 12.9517(4) Å	b = 8.7867(4) Å
	c = 10.214(3) Å	c = 6.4214(2) Å	c = 8.6139(4) Å
	α = 90.0°	α = 90.0°	α = 90.0°
	β = 100.260(10)°	β = 90.0°	β = 98.546(4)°
	γ = 90.0°	γ = 90.0°	γ = 90.0°
Volume ($Å^3$)	813.3(3)	1711.17(9)	915.96(8)
Z	2	4	2
Density (g/cm^3)	3.424	3.381	3.499

Table S3. Detailed calculation parameters of k-points with Γ-center meshes for sampling the Brillouin zones of the TMHP structures.

TMHP type	k-point setup
$(HEA)PbI_4$	4 × 4 × 3
$(MEA)_2PbI_4$	3 × 6 × 2
$(SEA)_2PbI_4$	2 × 3 × 3

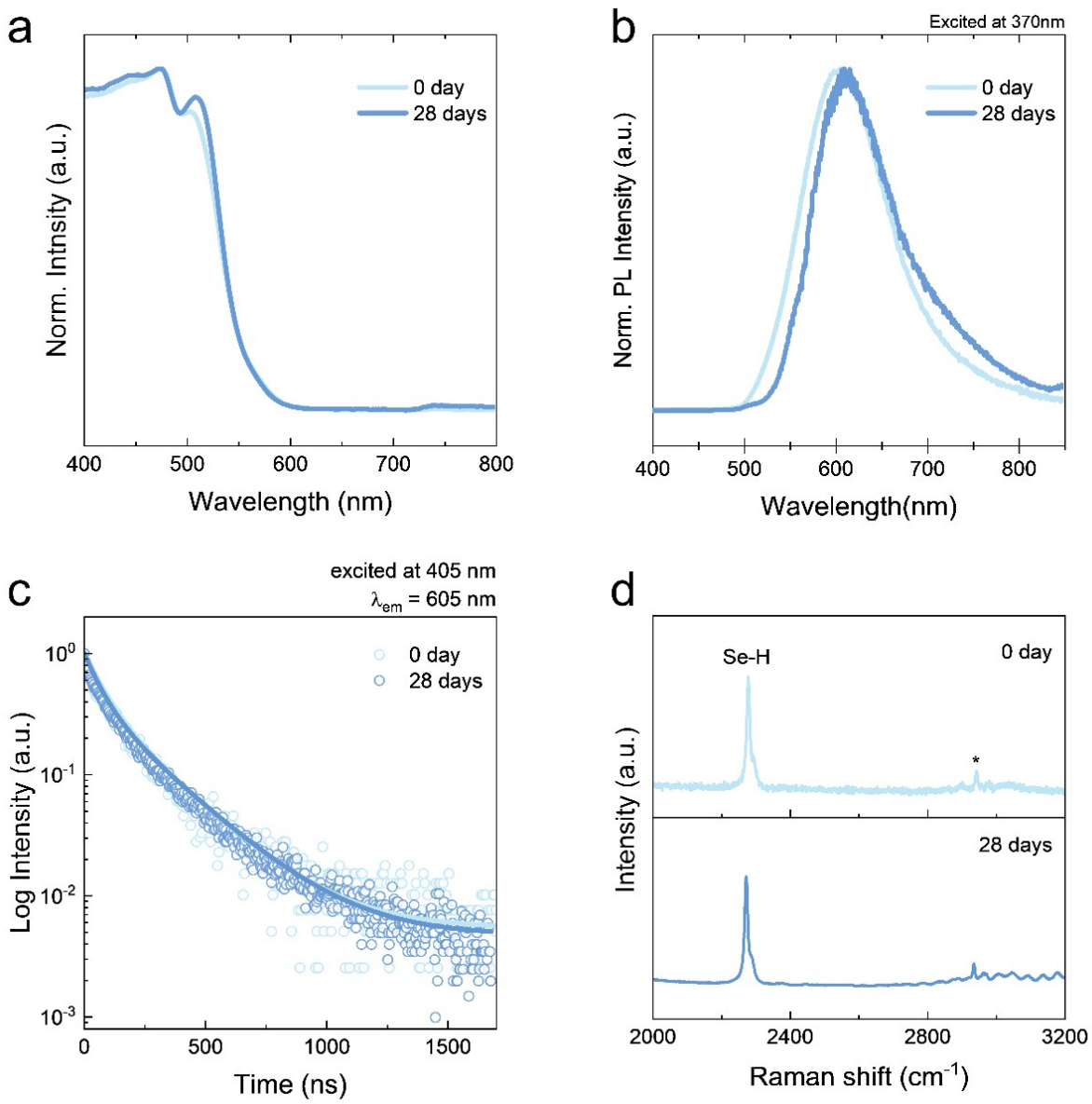

Figure S4. Stability characterization of $(SEA)_2PbI_4$ crystals. (a) Absorption spectra, **(b)** PL spectra, and **(c)** PL lifetimes decays (0-day: 183 ns; 28-day: 189 ns). **(d)** Raman spectra of $(SEA)_2PbI_4$ crystals before and after exposure for 28 days.

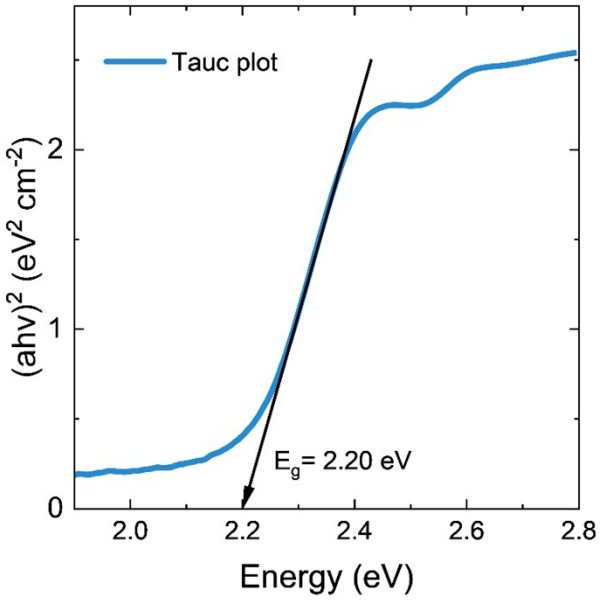

Figure S5. Tauc-plots of the optical absorption spectra of $(SEA)_2PbI_4$ shown in Figure 2e.

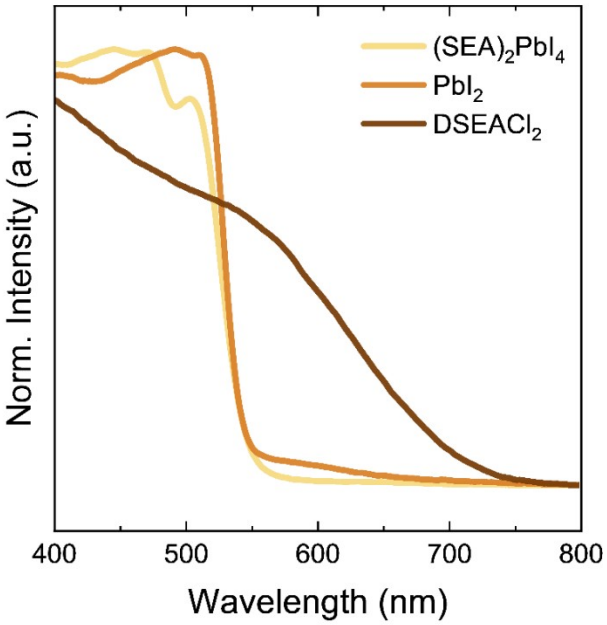

Figure S6. Normalized absorption spectra of the $(SEA)_2PbI_4$, PbI_2, and $DSEACl_2$.

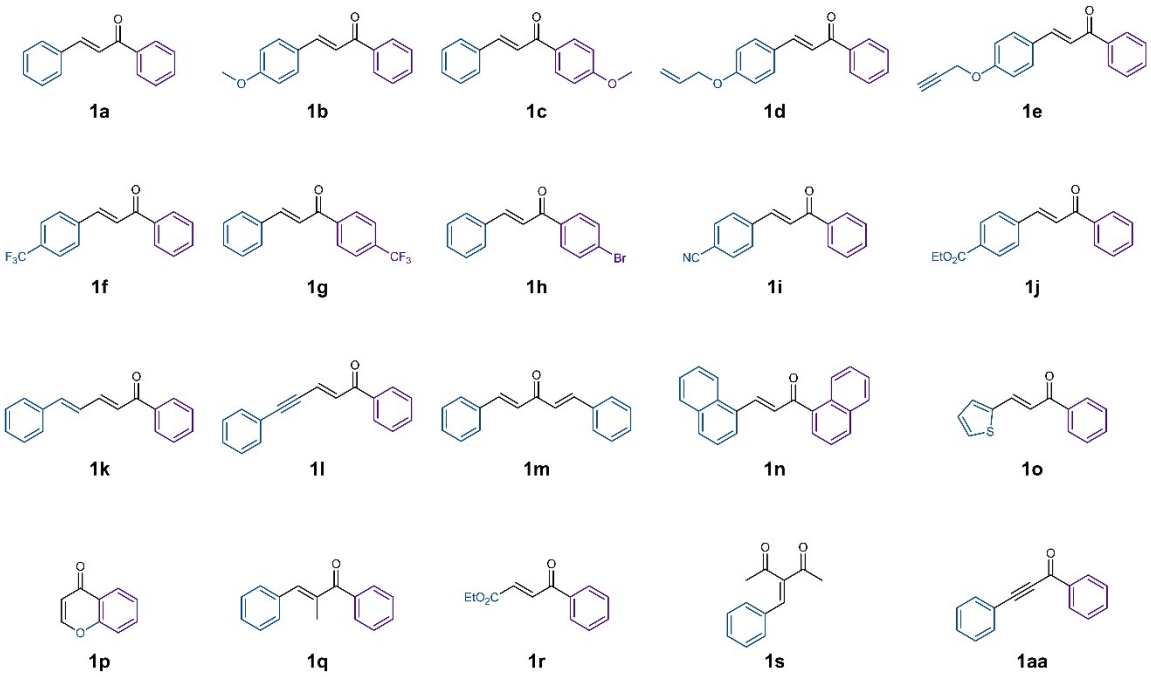

3. Substrates synthesis

Figure S7. Ketone substrates used in this study. Detailed preparation approaches are listed in Supplementary Section 2.1 – 2.7.

2.1 Materials

Chalcone (**1a**, 98%), ethanol (EtOH, 98%), sodium hydroxide (NaOH, 98%), sodium sulfate (Na_2SO_4, 99%), potassium carbonate (K_2CO_3, 99%), acetic acid (AcOH, 80%), tetrahydrofuran (THF, 99%), ethyl acetate (99%), *n*-butyllithium solution (*n*-BuLi, 1.3 mol/L in pentane), ammonium chloride (NH_4Cl, 99.5%), boron trifluoride diethyl etherate ($BF_3{\cdot}OEt_2$,95%), triethylamine (Et_3N, 99%), *p*-anisaldehyde (99%) and acetophenone (99%) was purchased from Sigma-Aldrich Inc. Ethyl 3-benzo-γ-pyrone (**1p**, 98%), benzoylacrylate (**1r**, 94%), 4-methoxyacetophenone (99%), benzaldehyde (98.5%), propargyl bromide (98%), and 4-hydroxy benzaldehyde (99%) was purchased from Macklin Inc. 4'-bromoacetophenone (98%), 4-formylbenzonitrile (98%), ethyl 4-formylbenzoate (95%), 1-naphthaldehyde (97%), 1-acetylnaphthalene (97%), 3-phenylpropiolaldehyde (95%), *trans*-cinnamaldehyde (98%), 2-thiophenecarboxaldehyde (98%), 4-(trifluoromethyl)benzaldehyde (97%), and 4'-(trifluoromethyl)acetophenone (98%) were purchased from Energy Chemical Inc. Allyl bromide (98%), 4'-bromoacetophenone (98%), and acetylacetone (99.6%) were purchased from Adamas Inc. Acetone (99.5%) and hydrochloric acid (HCl, 36.0 – 38.0 wt% in water) were purchased from Guangzhou Chemical Reagent Inc. Piperidine (99.5%) was purchased from Shanghai Hushi Chemical Co., Ltd. All chemicals used are commercially available and were used without any additional purification steps.

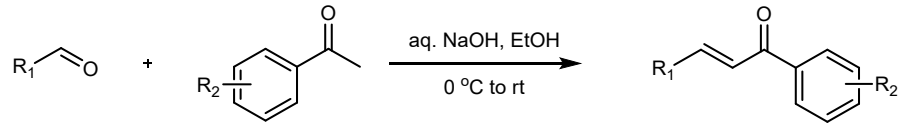

2.2 Preparation of 1b-1c, 1f-1k,1m-1n, and 1o.

α, *β*-Unsaturated ketones **1b-1c**, **1f-1 k,1m-1n,** and **1o** were synthesized via aldol condensation between benzaldehyde derivatives and aromatic ketones, following a modified literature procedure.[8] Briefly, a solution of the ketone substrate (5.0 mmol) in EtOH (10.0 mL) was cooled to 0 °C in a 50-mL round bottom flask, and aqueous NaOH (4.0 mL, 10 wt%) was added

dropwise with stirring. After stirred at 0 °C for 20 min, the mixture was stirred at room temperature for 1 h. The corresponding benzaldehyde derivative (5 mmol) was then added, and the reaction was monitored by thin layer chromatography (TLC) until the reaction was completed. The solvent was removed via rotary evaporation and the residue diluted with water and extracted with ethyl acetate (3 × 10 mL). The combined organic layers were dried over Na_2SO_4, followed by the concentration via rotary evaporation, and the residue was purified by silica gel chromatography to yield the desired *α*,*β*-unsaturated ketones **1b-1c**, **1f-1k**,**1m-1n**, and **1o**.

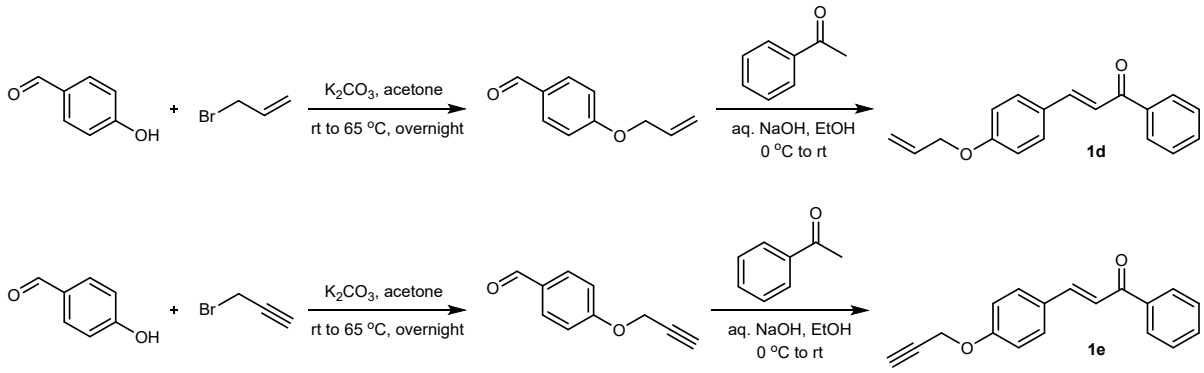

2.3 Preparation of 1d and 1e.

Compounds **1d** and **1e** were synthesized via a two-step procedure involving alkylation of phenols followed by aldol condensation, adapted from literature methods.[8,9] Briefly, in a 50 mL round-bottom flask, a mixture of 4-hydroxy benzaldehyde (1.0 mmol) and K_2CO_3 (1.5 mmol, in acetone (5.0 mL) was stirred at room temperature. Allyl bromide (or propargyl bromide, 1.1 mmol) in acetone (1.0 mL) was added dropwise, and the reaction was stirred for 30 min at room temperature before being heated to reflux at 65 °C overnight. The crude product was purified by silica gel chromatography to yield the corresponding benzaldehyde derivative.

A solution of acetophenone (1.0 mmol) in EtOH (3.0 mL) was cooled to 0 °C in a 50 mL flask, and aqueous NaOH (0.5 mL, 10 wt%) was added dropwise. After stirring at 0 °C for 20 min, the mixture was naturally was warmed to room temperature and kept stirring for 1 h. The pre-synthesized benzaldehyde derivative (1.0 mmol) was added, and the reaction was

monitored by TLC until completion. The solvent was evaporated via rotary evaporation, and the residue was diluted with water and extracted with ethyl acetate (3 × 10 mL). The combined organic layers were dried over Na_2SO_4, concentrated, and purified by silica gel chromatography to yield **1d** and **1e**.

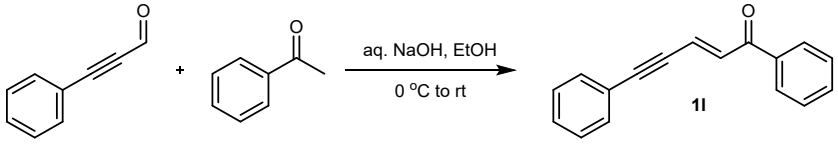

2.4 Preparation of 1l.

Compound **1l** was prepared via aldol condensation with 3-phenylpropiolaldehyde and acetophenone using NaOH as base, following a modified literature procedure.[10] In a 50-mL round-bottom flask, a solution of acetophenone (2.0 mmol) and 3-phenylpropiolaldehyde (2.0 mmol) in 6 mL of EtOH/water mixture (50 wt%) was cooled to 0 °C. 0.18 mL of NaOH aqueous solution (50 wt%) was added dropwise, followed by an addition 0.12 mL of diluted (20 wt%) NaOH aqueous solution upon precipitation. The solution was mechanically stirred at room temperature for 10 h. The resulting solid was collected by filtration, washed with cold 20 wt% EtOH/water mixture, and recrystallized from 70 – - 80 wt% EtOH/water mixture to yield compound **1l**.

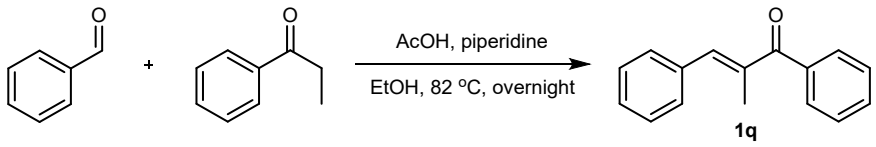

2.5 Preparation of 1q.

The synthesis of compound **1q** was achieved through aldol condensation of benzaldehyde and propiophenone according to literature method[11]. A mixture of in a 50 mL round-bottom flask, a mixture of propiophenone (5.0 mmol), benzaldehyde (5.0 mmol), piperidine (1.5 mL), and acetic acid (750 μL) in EtOH (8.0 mL) was refluxed at 82 °C until completion as monitored by TLC. After cooling to room temperature, the solvent was removed by rotary evaporation, and

the crude product was further purified by silica gel chromatography to yield compound **1q**.

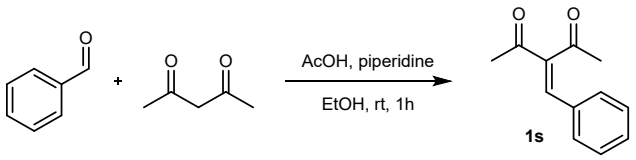

2.6 Preparation of 1s.

α, *β*-unsaturated ketone **1s** was prepared via aldol condensation between benzaldehyde and acetylacetone following established procedures.[12] A solution of benzaldehyde (2.0 mmol), acetylacetone (2.0 mmol), piperidine (2.0 mmol), and acetic acid (AcOH, 2.0 mmol) in EtOH (15.0 mL) was stirred at room temperature for 1 h. The reaction was quenched with ice water and extracted with ethyl acetate (3 × 10 mL). The combined organic layer was then washed with water, HCl (1 mol/L), and water again, then dried over dried over Na_2SO_4 and concentrated. The crude product was further purified by silica gel chromatography to yield compound **1s**.

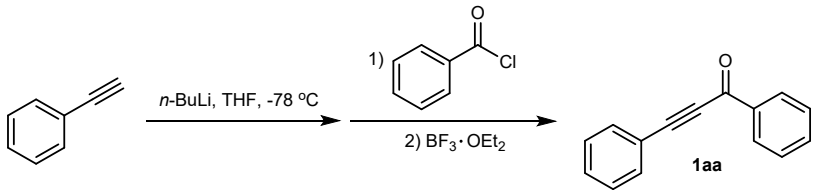

2.7 Preparation of 1aa.

Compund **1aa** was prepared via addition of lithium acetylide to benzoyl chloride according to literature procedures.[13] In a 50-mL round-bottom flask under nitrogen, a solution of morpholine (1.0 mmol) and phenylacetylene (3.0 mmol) in THF (5.0 mL) was cooled to -78 °C. *n*-BuLi (4.0 mmol) was added dropwise, and the mixture was stirred for 10 min at -78 °C. Benzoyl chloride (1.0 mmol) was then added dropwise, followed by $BF_3{\cdot}OEt_2$ (1.0 mmol), and the stirring continued for 30 min. The reaction was quenched with saturated NH_4Cl (10 mL) and extracted with ethyl acetate (3 × 10 mL). The combined organic layer was dried over Na_2SO_4, concentrated, and purified by silica gel chromatography (eluent containing Et_3N) to yield **1aa**.

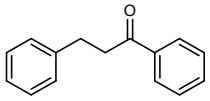

4. Summary of NMR data

1,3-Diphenylpropan-1-one (2a)[14]

Preparative thin layer chromatography (eluent: PE/EA = 20:1, v/v) to afford **2a** as a white solid (15.8 mg, 75%). R_f = 0.3 (PE/EA = 20:1, v/v).

^{1}H NMR (400 MHz, $CDCl_3$) δ 7.99 – 7.91 (m, 2H), 7.54 (t, *J* = 7.4 Hz, 1H), 7.44 (t, *J* = 7.7 Hz, 2H), 7.33 – 7.27 (m, 2H), 7.27 – 7.23 (m, 2H), 7.20 (t, *J* = 7.0 Hz, 1H), 3.33 – 3.26 (m, 2H), 3.10 – 3.03 (m, 2H).

^{13}C NMR (101 MHz, $CDCl_3$) δ 199.3, 141.4, 137.0, 133.2, 128.7, 128.6, 128.5, 128.2, 126.3, 40.5, 30.3.

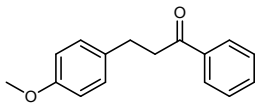

3-(4-Methoxyphenyl)-1-phenylpropan-1-one (2b)[14]

Preparative thin layer chromatography (eluent: PE/EA = 20:1, v/v) to afford **2b** as a yellow solid (19.4 mg, 81%). R_f = 0.2 (PE/EA = 20:1, v/v).

^{1}H NMR (400 MHz, $CDCl_3$) δ 8.02 – 7.90 (m, 2H), 7.54 (d, *J* = 7.3 Hz, 1H), 7.45 (t, *J* = 7.6 Hz, 2H), 7.17 (d, *J* = 8.4 Hz, 2H), 6.89 – 6.79 (m, 2H), 3.79 (s, 3H), 3.27 (dd, *J* = 8.3, 7.0 Hz, 2H), 3.02 (t, *J* = 7.6 Hz, 2H).

^{13}C NMR (101 MHz, $CDCl_3$) δ 199.5, 158.2, 137.1, 133.5, 133.2, 129.5, 128.7, 128.2, 114.1, 55.4, 40.9, 29.5.

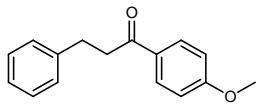

1-(4-Methoxyphenyl)-3-phenylpropan-1-one (2c)[14]

Preparative thin layer chromatography (eluent: PE/EA = 20:1, v/v) to afford **2c** as a light-yellow solid (18.7 mg, 78%). R_f = 0.2 (PE/EA = 20:1, v/v).

^{1}H NMR (400 MHz, $CDCl_3$) δ 7.94 (d, *J* = 8.6 Hz, 2H), 7.33 – 7.17 (m, 5H), 6.93 (d, *J* = 8.7 Hz, 2H), 3.87 (s, 3H), 3.25 (t, *J* = 7.7 Hz, 2H), 3.06 (t, *J* = 7.7 Hz, 2H).

^{13}C NMR (101 MHz, $CDCl_3$) δ 198.0, 163.6, 141.6, 130.5, 130.2, 128.65, 128.57, 126.2, 113.9, 55.6, 40.3, 30.5.

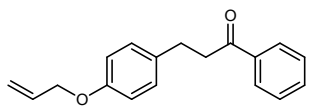

3-(4-(Allyloxy)phenyl)-1-phenylpropan-1-one (2d)[15]

Preparative thin layer chromatography (eluent: PE/EA = 100:1, v/v) to afford **2d** as a colorless oil (14.9 mg, 56%). R_f = 0.5 (PE/EA = 100:1, v/v).

^{1}H NMR (400 MHz, $CDCl_3$) δ 8.04 – 7.86 (m, 2H), 7.55 (t, *J* = 7.1 Hz, 1H), 7.45 (t, *J* = 7.4 Hz, 2H), 7.16 (d, *J* = 8.1 Hz, 2H), 6.86 (d, *J* = 8.2 Hz, 2H), 6.05 (ddt, *J* = 16.2, 10.4, 5.4 Hz, 1H), 5.40 (d, *J* = 18.9 Hz, 1H), 5.28 (d, *J* = 10.4 Hz, 1H), 4.57 – 4.46 (m, 2H), 3.27 (t, *J* = 7.6 Hz, 2H), 3.01 (t, *J* = 7.7 Hz, 2H).

^{13}C NMR (101 MHz, $CDCl_3$) δ 199.6, 157.2, 137.1, 133.7, 133.6, 133.2, 129.5, 128.7, 128.2, 117.7, 115.0, 69.0, 40.8, 29.5.

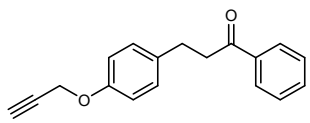

1-Phenyl-3-(4-(prop-2-yn-1-yloxy)phenyl)propan-1-one (2e)

Preparative thin layer chromatography (eluent: PE/EA = 20:1, v/v) to afford **2e** as a colorless

oil (14.0 mg, 53%). R_f = 0.5 (PE/EA = 20:1, v/v).

^{1}H NMR (400 MHz, $CDCl_3$) δ 7.95 (d, *J* = 7.2 Hz, 2H), 7.55 (t, *J* = 7.2 Hz, 1H), 7.45 (t, *J* = 7.5 Hz, 2H), 7.19 (d, *J* = 8.3 Hz, 2H), 6.92 (d, *J* = 8.7 Hz, 2H), 4.67 (d, *J* = 2.5 Hz, 2H), 3.27 (t, *J* = 7.6 Hz, 2H), 3.02 (t, *J* = 7.7 Hz, 2H), 2.51 (s, 1H).

^{13}C NMR (101 MHz, $CDCl_3$) δ 199.5, 156.1, 137.1, 134.5, 133.2, 129.5, 128.7, 128.2, 115.2, 78.9, 75.5, 56.0, 40.7, 29.4.

HRMS (APCI): (*m*/*z*) Calculated for $C_{18}H_{17}O_2^+$ $[M+H]^+$ 265.1223; Found 265.1225.

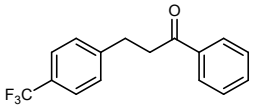

1-Phenyl-3-(4-(trifluoromethyl)phenyl)propan-1-one (2f)[16]

Preparative thin layer chromatography (eluent: PE/EA = 10:1, v/v) to afford **2f** as a light-yellow oil (13.1 mg, 47%). R_f = 0.5 (PE/EA = 10:1, v/v).

^{1}H NMR (400 MHz, $CDCl_3$) δ 7.96 (d, *J* = 7.2 Hz, 2H), 7.56 (dd, *J* = 11.5, 7.8 Hz, 3H), 7.46 (t, *J* = 7.6 Hz, 2H), 7.37 (d, *J* = 8.0 Hz, 2H), 3.33 (t, *J* = 7.4 Hz, 2H), 3.14 (t, *J* = 7.4 Hz, 2H).

^{13}C NMR (101 MHz, $CDCl_3$) δ 198.7, 145.6, 136.8, 133.4, 128.9, 128.8, 128.5, 128.1, 125.6 (q, *J* = 11.1 Hz), 124.4 (q, *J* = 272.0 Hz), 40.0, 29.9.

^{19}F NMR (376 MHz, $CDCl_3$) δ -62.39.

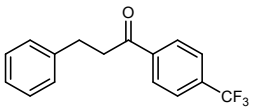

3-Phenyl-1-(4-(trifluoromethyl)phenyl)propan-1-one (2g)[17]

Preparative thin layer chromatography (eluent: PE/EA = 20:1, v/v) to afford **2g** as a light-yellow oil (10.3 mg, 37%). R_f = 0.4 (PE/EA = 20:1, v/v).

^{1}H NMR (400 MHz, $CDCl_3$) δ 8.05 (d, *J* = 8.1 Hz, 2H), 7.72 (d, *J* = 8.2 Hz, 2H), 7.35 – 7.28

(m, 2H), 7.26 – 7.18 (m, 3H), 3.33 (t, J = 7.6 Hz, 2H), 3.09 (t, J = 7.6 Hz, 2H).

^{13}C NMR (101 MHz, $CDCl_3$) δ 198.3, 141.0, 139.6, 134.5 (q, J = 32.6 Hz), 128.8, 128.6, 128.5, 126.4, 125.9 (q, J = 3.7 Hz), 123.7 (q, J = 273.7 Hz), 40.9, 30.1.

^{19}F NMR (376 MHz, $CDCl_3$) δ -63.12.

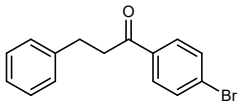

1-(4-Bromophenyl)-3-phenylpropan-1-one (2h)[14]

Preparative thin layer chromatography (eluent: PE/EA = 20:1, v/v) to afford **2h** as a white sold (18.7 mg, 65%). R_f = 0.3 (PE/EA = 20:1, v/v).

^{1}H NMR (400 MHz, $CDCl_3$) δ 7.82 (d, J = 8.2 Hz, 2H), 7.60 (d, J = 8.3 Hz, 2H), 7.31 (t, J = 7.5 Hz, 2H), 7.27 – 7.19 (m, 3H), 3.27 (t, J = 7.6 Hz, 2H), 3.07 (t, J = 7.6 Hz, 2H).

^{13}C NMR (101 MHz, $CDCl_3$) δ 198.3, 141.2, 135.7, 132.1, 129.7, 128.7, 128.5, 128.4, 126.4, 40.5, 30.2.

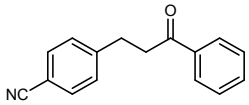

4-(3-Oxo-3-phenylpropyl)benzonitrile (2i)[18]

Preparative thin layer chromatography (eluent: PE/EA = 15:1, v/v) to afford **2i** as a colorless oil (15.8 mg, 67%). R_f = 0.5 (PE/EA = 15:1, v/v).

^{1}H NMR (400 MHz, $CDCl_3$) δ 7.94 (d, J = 7.1 Hz, 2H), 7.57 (t, J = 7.1 Hz, 3H), 7.46 (t, J = 7.6 Hz, 2H), 7.37 (d, J = 7.9 Hz, 2H), 3.32 (t, J = 7.3 Hz, 2H), 3.14 (t, J = 7.3 Hz, 2H).

^{13}C NMR (101 MHz, $CDCl_3$) δ 198.4, 147.1, 136.7, 133.5, 132.5, 129.5, 128.8, 128.1, 119.1, 110.2, 39.6, 30.1.

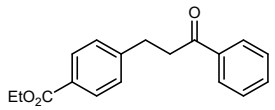

Ethyl 4-(3-oxo-3-phenylpropyl)benzoate (2j)[19]

Preparative thin layer chromatography (eluent: PE/EA = 40:1, v/v) to afford **2j** as a colorless oil (17.2 mg, 61%). R_f = 0.5 (PE/EA = 40:1, v/v).

^{1}H NMR (400 MHz, $CDCl_3$) δ 7.96 (t, *J* = 8.2 Hz, 4H), 7.60 – 7.52 (m, 1H), 7.45 (t, *J* = 7.6 Hz, 2H), 7.32 (d, *J* = 8.0 Hz, 2H), 4.36 (q, *J* = 7.1 Hz, 2H), 3.32 (t, *J* = 7.5 Hz, 2H), 3.13 (t, *J* = 7.5 Hz, 2H), 1.38 (t, *J* = 7.1 Hz, 3H).

^{13}C NMR (101 MHz, $CDCl_3$) δ 198.8, 166.7, 146.8, 136.9, 133.3, 130.0, 128.8, 128.7, 128.6, 128.2, 61.0, 40.0, 30.2, 14.5.

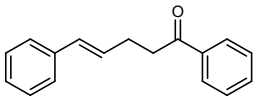

(E)-1,5-diphenylpent-4-en-1-one (2k)[20]

Preparative thin layer chromatography (eluent: PE/EA = 20:1, v/v) to afford **2m** as a light-yellow solid (16.3 mg, 69%). R_f = 0.5 (PE/EA = 20:1, v/v).

^{1}H NMR (400 MHz, $CDCl_3$) δ 7.98 (d, *J* = 7.0 Hz, 2H), 7.57 (t, *J* = 7.4 Hz, 1H), 7.47 (t, *J* = 7.5 Hz, 2H), 7.38 – 7.32 (m, 2H), 7.29 (t, *J* = 7.6 Hz, 2H), 7.20 (d, *J* = 7.2 Hz, 1H), 6.47 (d, *J* = 15.9 Hz, 1H), 6.30 (dt, *J* = 15.8, 6.8 Hz, 1H), 3.16 (t, *J* = 7.3 Hz, 2H), 2.67 (q, *J* = 6.9 Hz, 2H).

^{13}C NMR (101 MHz, $CDCl_3$) δ 199.5, 137.6, 137.1, 133.2, 131.0, 129.3, 128.8, 128.6, 128.2, 127.2, 126.2, 38.4, 27.7.

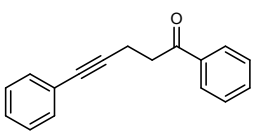

1,5-Diphenylpent-4-yn-1-one (2l)[21]

Preparative thin layer chromatography (eluent: PE/EA = 20:1, v/v) to afford **2n** as a yellow solid (8.4 mg, 36%). R_f = 0.5 (PE/EA = 20:1, v/v).

^{1}H NMR (400 MHz, $CDCl_3$) δ 8.02 – 7.97 (m, 2H), 7.60 – 7.56 (m, 1H), 7.48 (ddd, *J* = 8.3, 6.6, 1.3 Hz, 2H), 7.40 – 7.35 (m, 2H), 7.28 – 7.26 (m, 3H), 3.36 – 3.29 (m, 2H), 2.90 – 2.82 (m, 2H).

^{13}C NMR (101 MHz, $CDCl_3$) δ 198.2, 136.7, 133.4, 131.7, 128.8, 128.3, 128.2, 127.9, 123.8, 89.0, 81.2, 38.0, 14.5.

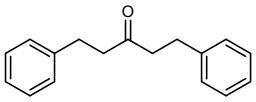

1,5-Diphenylpentan-3-one (2m)[22]

Preparative thin layer chromatography (eluent: PE/EA = 20:1, v/v) to afford **2l** as a yellow oil (12.9 mg, 54%). R_f = 0.5 (PE/EA = 20:1, v/v).

^{1}H NMR (400 MHz, $CDCl_3$) δ 7.25 – 7.21 (m, 4H), 7.15 (dd, *J* = 17.7, 7.3 Hz, 6H), 2.86 (t, *J* = 7.6 Hz, 4H), 2.68 (t, *J* = 7.6 Hz, 4H).

^{13}C NMR (101 MHz, $CDCl_3$) δ 209.2, 141.2, 128.6, 128.5, 126.3, 44.7, 29.9.

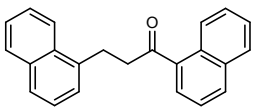

1,3-Di(naphthalen-1-yl)propan-1-one (2n)[23]

Preparative thin layer chromatography (eluent: PE/EA = 20:1, v/v) to afford **2k** as a colorless oil (22.0 mg, 71%). R_f = 0.6 (PE/EA = 20:1, v/v).

^{1}H NMR (400 MHz, $CDCl_3$) δ 8.65 (d, *J* = 8.5 Hz, 1H), 8.10 (d, *J* = 8.2 Hz, 1H), 7.97 (d, *J* = 8.3 Hz, 1H), 7.88 (d, *J* = 8.0 Hz, 2H), 7.81 (d, *J* = 7.2 Hz, 1H), 7.78 – 7.70 (m, 1H), 7.61 (d, *J* = 6.6 Hz, 1H), 7.58 – 7.47 (m, 3H), 7.43 (q, *J* = 7.3 Hz, 3H), 3.63 (t, *J* = 7.2 Hz, 2H), 3.57 – 3.45 (m, 2H).

^{13}C NMR (101 MHz, $CDCl_3$) δ 203.6, 137.3, 136.0, 134.13, 134.11, 132.8, 131.8, 130.3, 129.1, 128.6, 128.1, 127.7, 127.2, 126.6, 126.3, 126.2, 126.0, 125.8, 125.7, 124.5, 123.7, 43.2, 27.9.

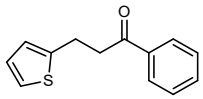

1-Phenyl-3-(thiophen-2-yl)propan-1-one (2o)[18]

Preparative thin layer chromatography (eluent: PE/EA = 20:1, v/v) to afford **2o** as a colorless oil (14.3 mg, 66%). R_f = 0.3 (PE/EA = 20:1, v/v).

^{1}H NMR (400 MHz, $CDCl_3$) δ 7.97 (d, *J* = 6.8 Hz, 2H), 7.57 (t, *J* = 7.2 Hz, 1H), 7.47 (t, *J* = 7.6 Hz, 2H), 7.13 (d, *J* = 5.0 Hz, 1H), 6.92 (dd, *J* = 5.2, 3.3 Hz, 1H), 6.87 (s, 1H), 3.40 – 3.34 (m, 2H), 3.33 – 3.27 (m, 2H).

^{13}C NMR (101 MHz, $CDCl_3$) δ 198.7, 144.0, 136.9, 133.3, 128.8, 128.2, 127.0, 124.8, 123.5, 40.7, 24.4.

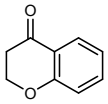

Chroman-4-one (2p)[20]

Preparative thin layer chromatography (eluent: PE/EA = 20:1, v/v) to afford **2p** as a yellow oil (10.2 mg, 69%). R_f = 0.4 (PE/EA = 20:1, v/v).

^{1}H NMR (400 MHz, $CDCl_3$) δ 7.90 (d, *J* = 7.9 Hz, 1H), 7.47 (t, *J* = 7.0 Hz, 1H), 7.13 – 6.87 (m, 2H), 4.54 (t, *J* = 6.5 Hz, 2H), 2.82 (t, *J* = 6.5 Hz, 2H).

^{13}C NMR (101 MHz, $CDCl_3$) δ 191.9, 162.0, 136.1, 127.3, 121.54, 121.53, 118.0, 67.2, 38.0.

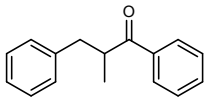

2-Methyl-1,3-diphenylpropan-1-one (2q)[24]

Preparative thin layer chromatography (eluent: PE/EA = 30:1, v/v) to afford **2q** as a yellow oil

(7.8 mg, 35%). R_f = 0.4 (PE/EA = 30:1, v/v).

^{1}H NMR (400 MHz, $CDCl_3$) δ 8.02 (d, *J* = 7.0 Hz, 2H), 7.64 (t, *J* = 7.4 Hz, 1H), 7.55 (t, *J* = 7.6 Hz, 2H), 7.39 – 7.27 (m, 5H), 3.85 (dq, *J* = 13.5, 6.9 Hz, 1H), 3.27 (dd, *J* = 13.7, 6.3 Hz, 1H), 2.80 (dd, *J* = 13.7, 7.8 Hz, 1H), 1.31 (d, *J* = 6.9 Hz, 3H).

^{13}C NMR (101 MHz, $CDCl_3$) δ 203.9, 140.1, 136.6, 133.1, 129.2, 128.8, 128.5, 128.4, 126.3, 42.9, 39.5, 17.5.

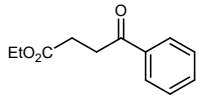

Ethyl 4-oxo-4-phenylbutanoate (2r)[17]

Preparative thin layer chromatography (eluent: PE/EA = 20:1, v/v) to afford **2r** as a colorless oil (6.2 mg, 30%). R_f = 0.3 (PE/EA = 20:1, v/v).

^{1}H NMR (400 MHz, $CDCl_3$) δ 7.99 (d, *J* = 7.5 Hz, 2H), 7.57 (t, *J* = 7.3 Hz, 1H), 7.47 (t, *J* = 7.6 Hz, 2H), 4.16 (q, *J* = 7.1 Hz, 2H), 3.31 (t, *J* = 6.7 Hz, 2H), 2.76 (t, *J* = 6.7 Hz, 2H), 1.27 (t, *J* = 7.1 Hz, 3H).

^{13}C NMR (101 MHz, $CDCl_3$) δ 198.3, 173.1, 136.8, 133.3, 128.8, 128.2, 60.8, 33.6, 28.5, 14.3.

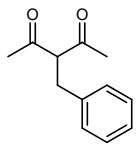

3-Benzylpentane-2,4-dione (2s)[25]

Preparative thin layer chromatography (eluent: PE/EA = 20:1, v/v) to afford **2s** as a colorless oil (13.9 mg, 73%). R_f = 0.5 (PE/EA =20:1, v/v).

^{1}H NMR (400 MHz, 2.12:1 enol:keto tautomer, keto tautomer annoted by an asterisk, $CDCl_3$) δ 16.80 (s, 1H), 7.34 – 7.26 (m, 6H), 7.24 – 7.11 (m, 10H), 4.00 (t, *J* = 7.5 Hz, 2H), 3.66 (s, 2H), 3.15 (d, *J* = 7.5 Hz, 4H), 2.12 (s, 13H), 2.07 (s, 6H).

^{13}C NMR (101 MHz, $CDCl_3$) δ 203.7, 192.1, 139.8, 138.1, 128.9, 128.8, 128.7, 127.6, 126.9, 126.5, 108.4, 70.1, 34.4, 33.0, 29.9, 23.4.

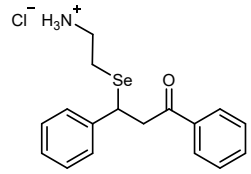

2-((3-oxo-1,3-diphenylpropyl)selanyl)ethan-1-aminium chloride (II)

^{1}H NMR (400 MHz, DMSO-d_6) δ 8.02 – 7.98 (m, 2H), 7.64 (t, J = 7.4 Hz, 1H), 7.52 (t, J = 7.6 Hz, 2H), 7.46 (d, J = 7.6 Hz, 2H), 7.29 (t, J = 7.5 Hz, 2H), 7.19 (t, J = 7.3 Hz, 1H), 5.90 (s, 2H), 4.70 (t, J = 7.3 Hz, 1H), 3.99 – 3.77 (m, 2H), 2.89 (td, J = 10.2, 5.8 Hz, 2H), 2.75 – 2.58 (m, 2H).

^{13}C NMR (101 MHz, DMSO-d_6) δ 197.5, 142.8, 136.5, 133.6, 128.9, 128.5, 128.2, 127.7, 127.0, 44.1, 37.3, 20.3.

HRMS (APCI): (*m*/*z*) Calculated for $C_{17}H_{20}NOSe^+$ $[M\text{-}Cl]^+$ 334.0705; Found 334.0704.

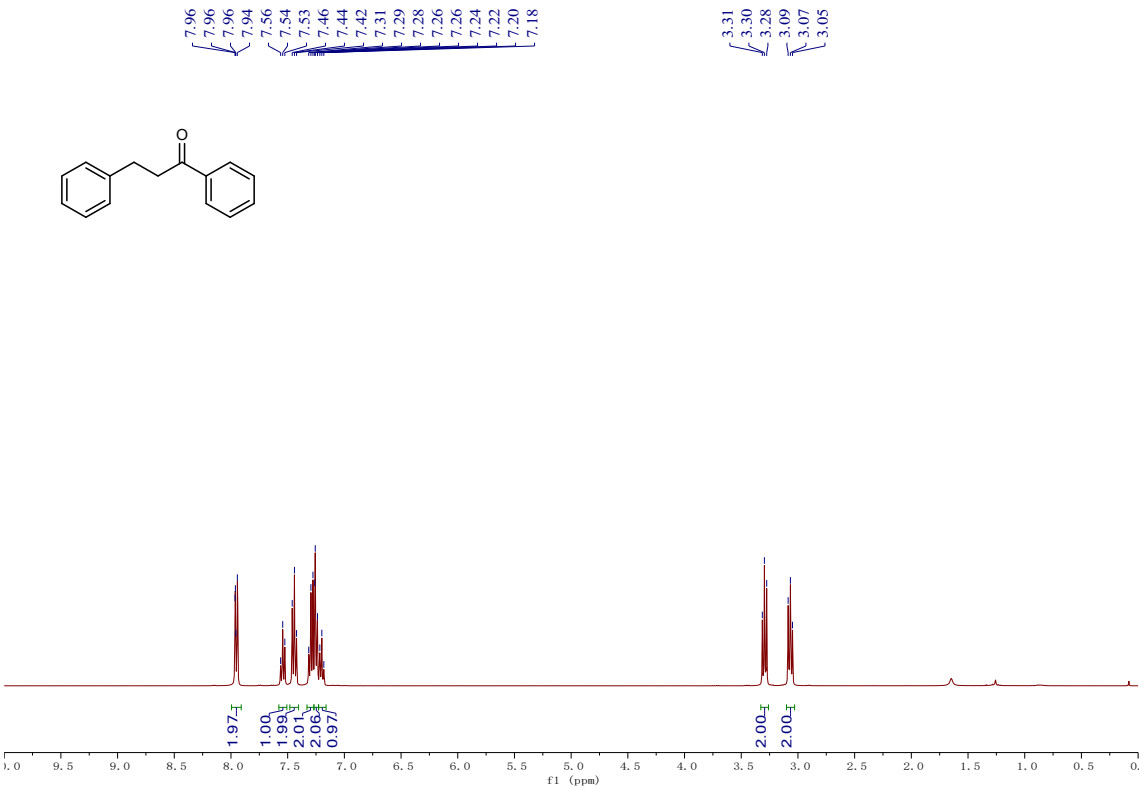

5. Supplementary NMR spectra for products

Figure S8. ^{1}H NMR (400 MHz, $CDCl_3$) spectrum of compound 2a.

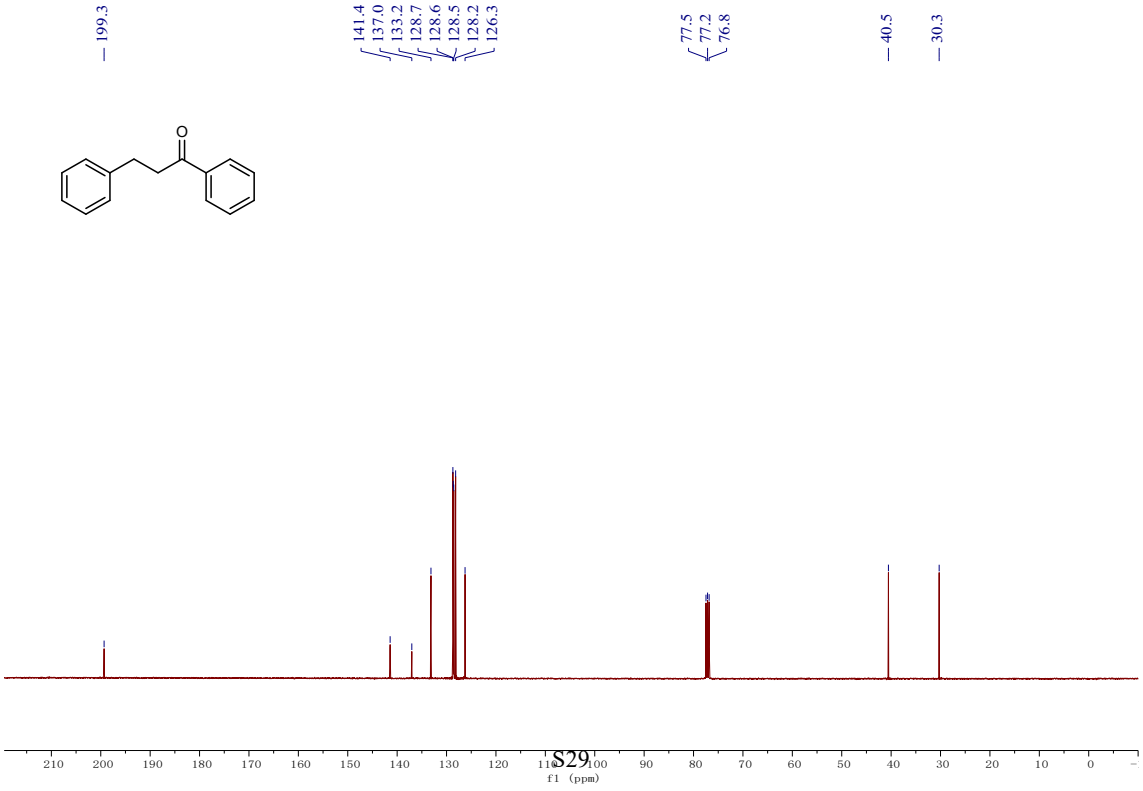

Figure S9. ^{13}C NMR (101 MHz, $CDCl_3$) spectrum of compound 2a.

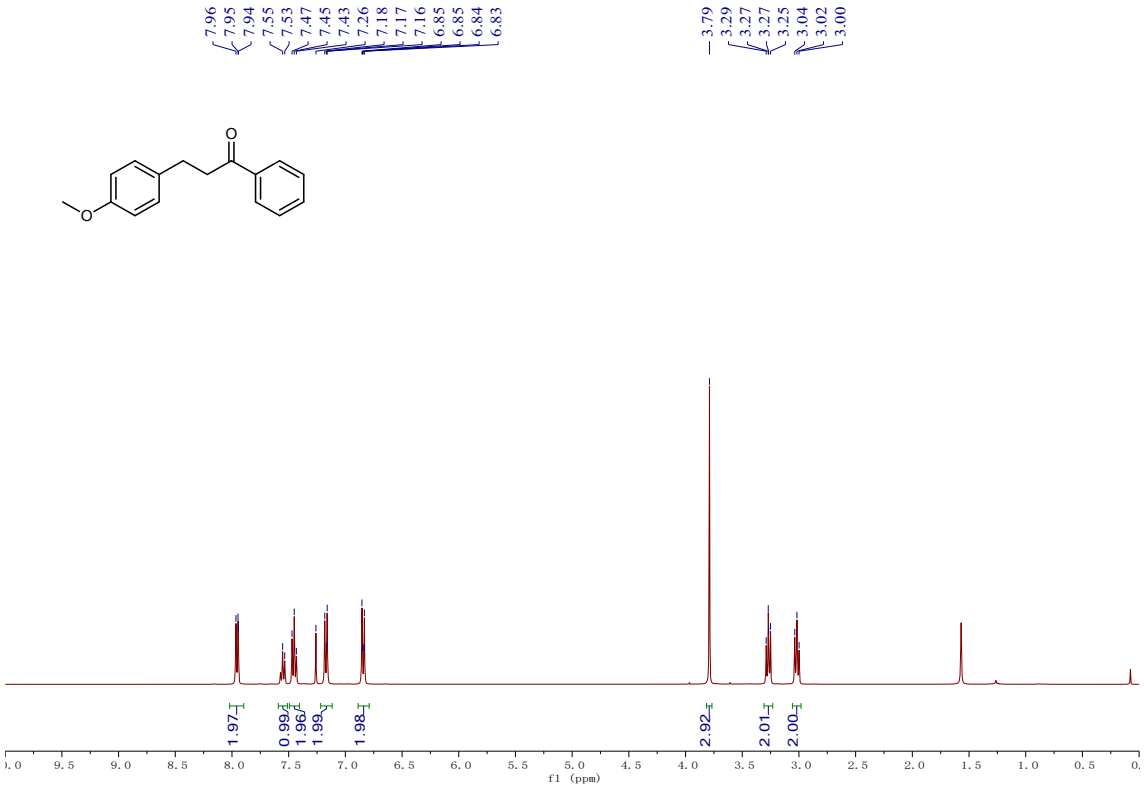

Figure S10. ^{1}H NMR (400 MHz, $CDCl_3$) spectrum of compound 2b.

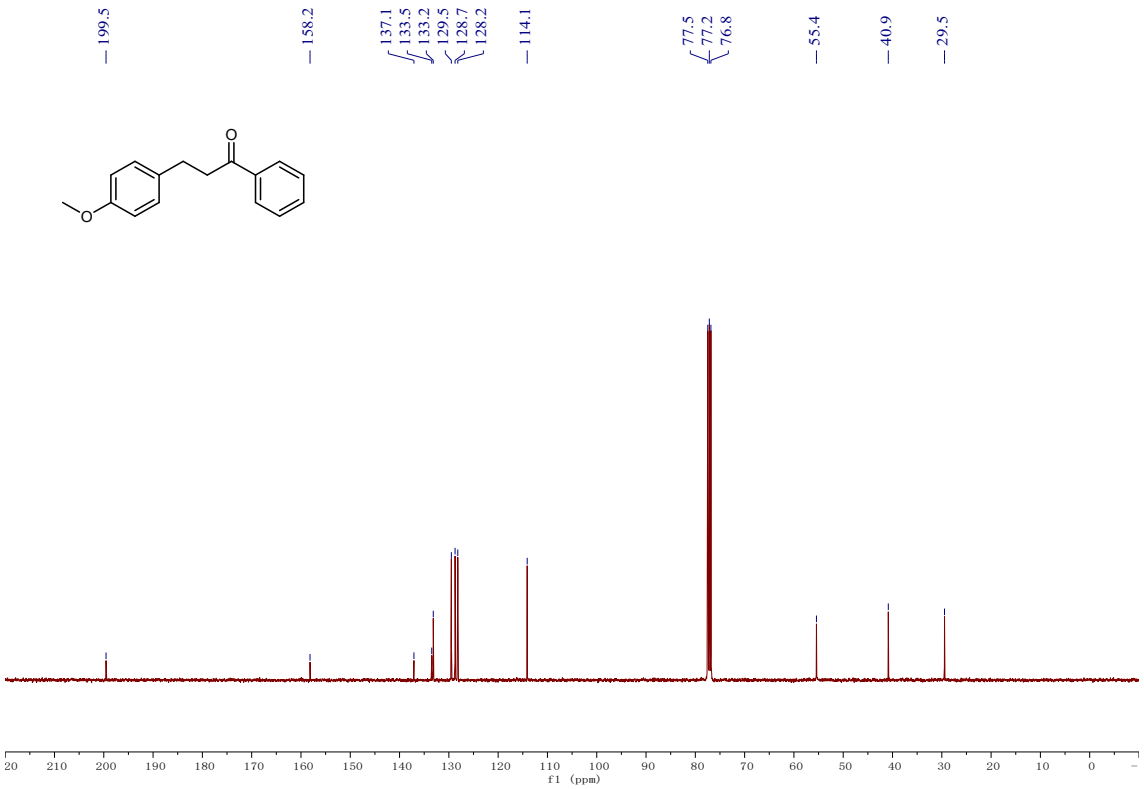

Figure S11. ^{13}C NMR (101 MHz, $CDCl_3$) spectrum of compound 2b.

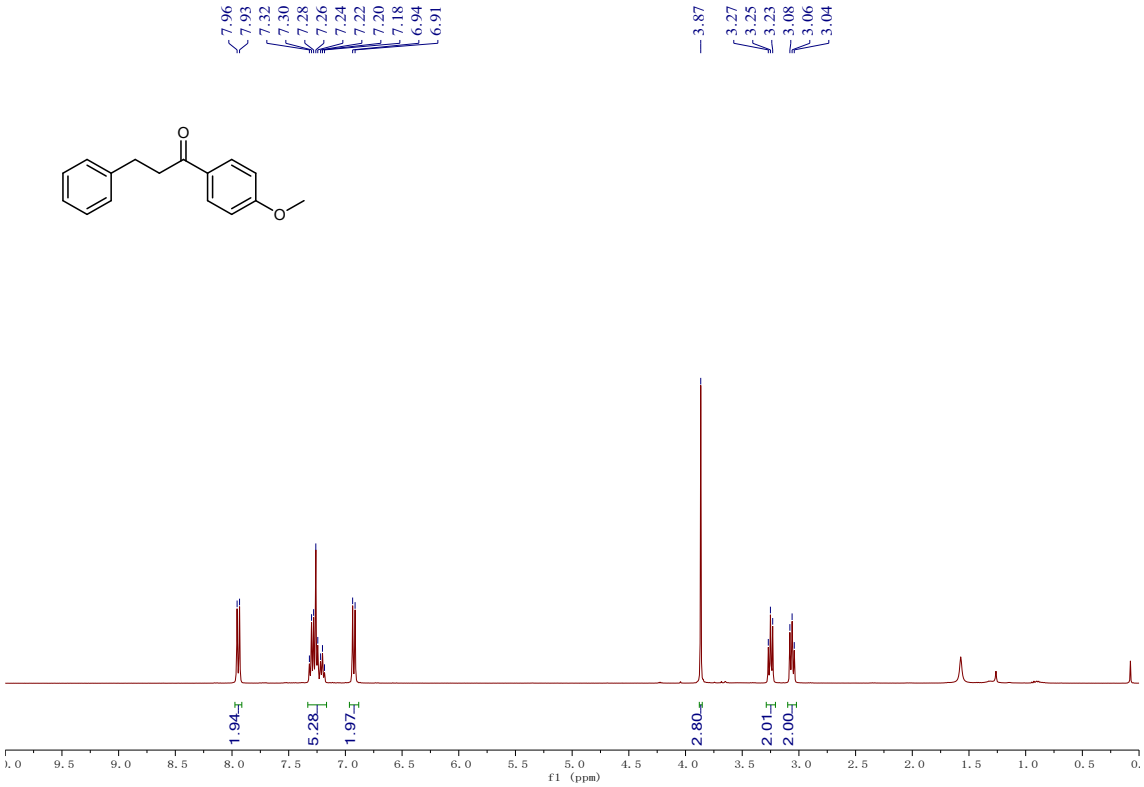

Figure S12. ^{1}H NMR (400 MHz, $CDCl_3$) spectrum of compound 2c.

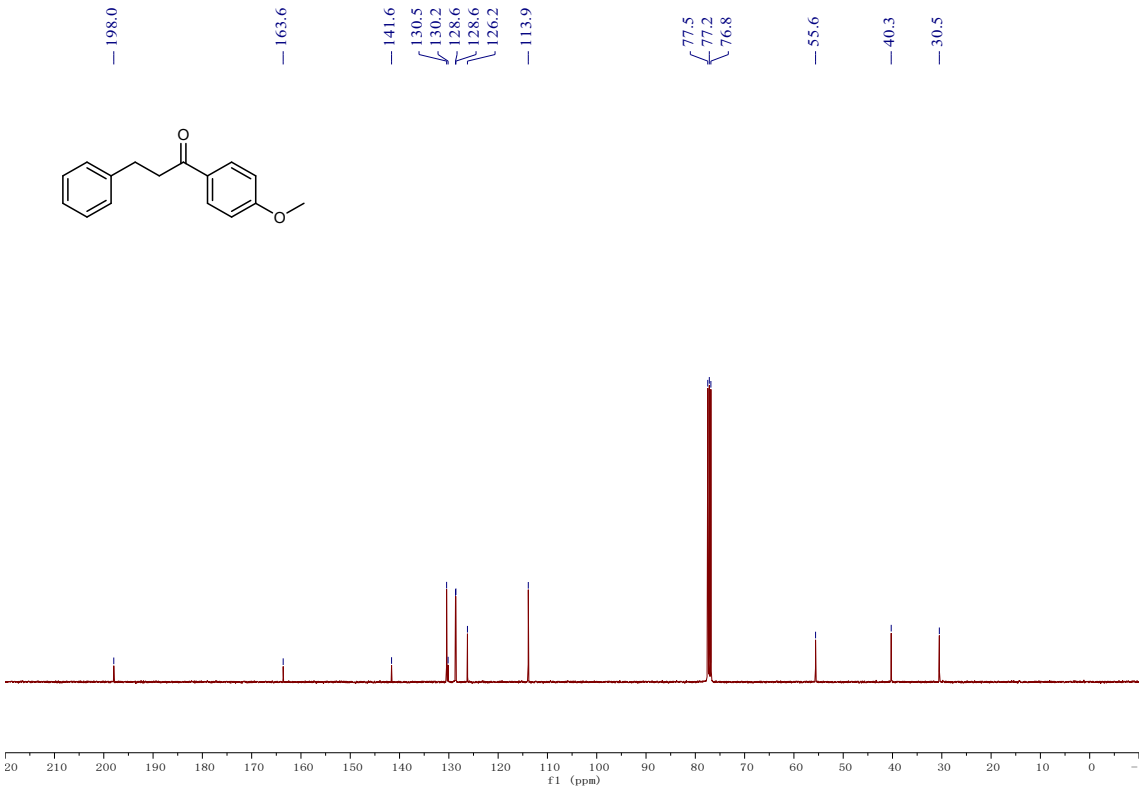

Figure S13. ^{13}C NMR (101 MHz, $CDCl_3$) spectrum of compound 2c.

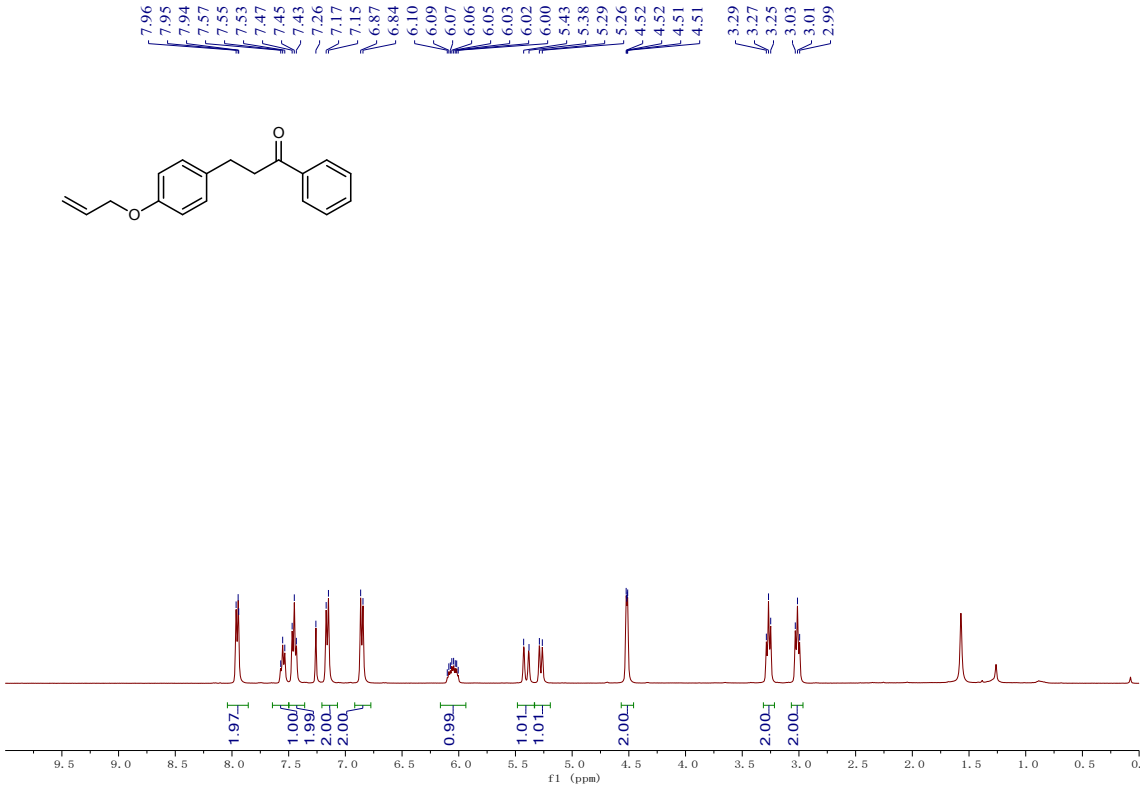

Figure S14. ^{1}H NMR (400 MHz, $CDCl_3$) spectrum of compound 2d.

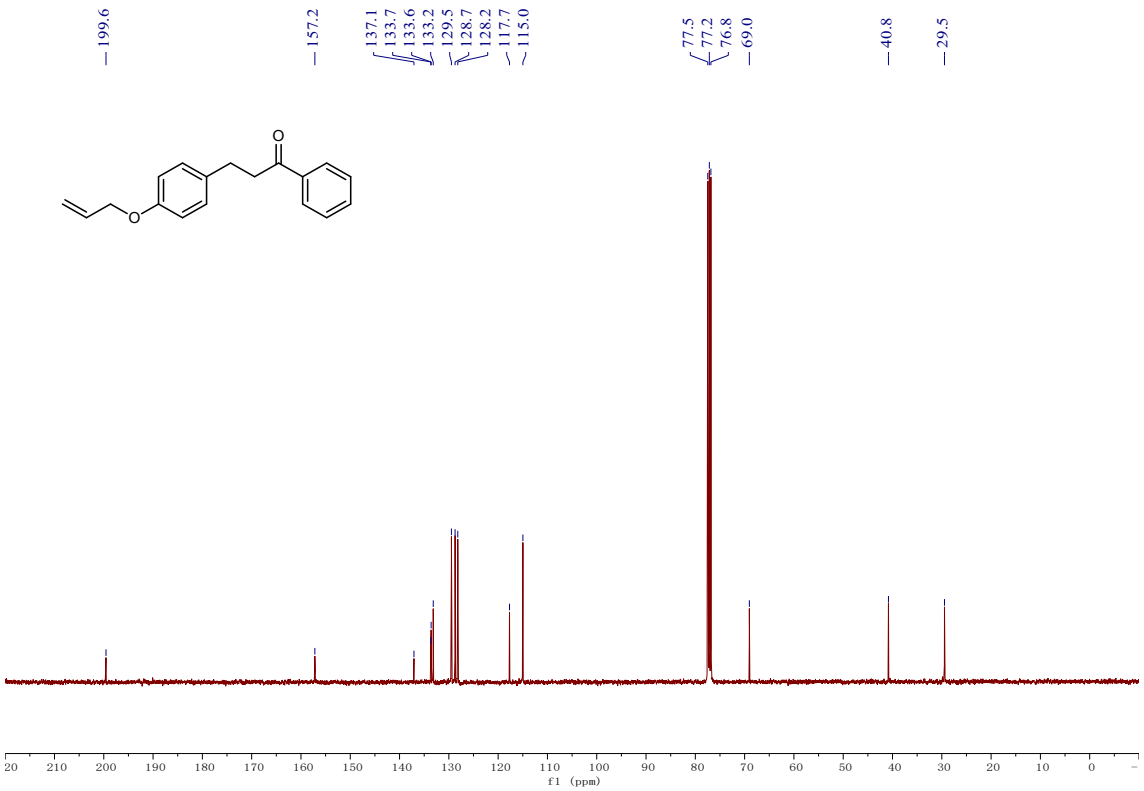

Figure S15. ^{13}C NMR (101 MHz, $CDCl_3$) spectrum of compound 2d.

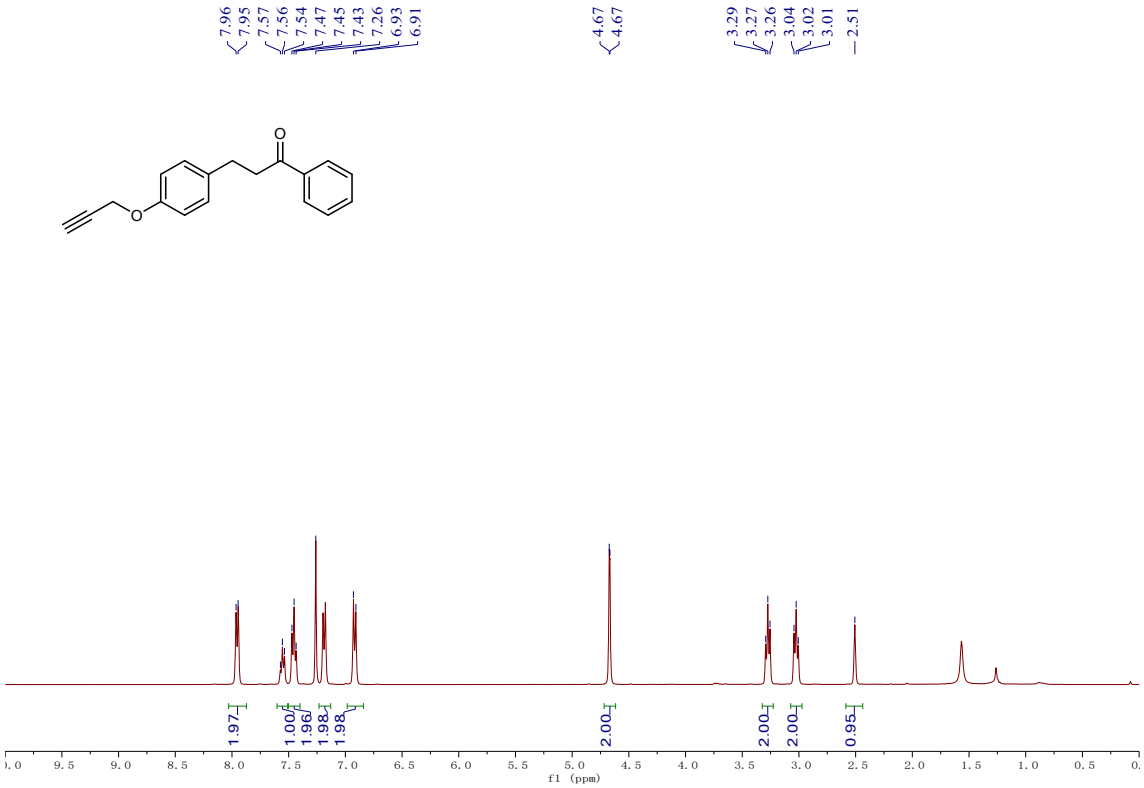

Figure S16. ^{1}H NMR (400 MHz, $CDCl_3$) spectrum of compound 2e.

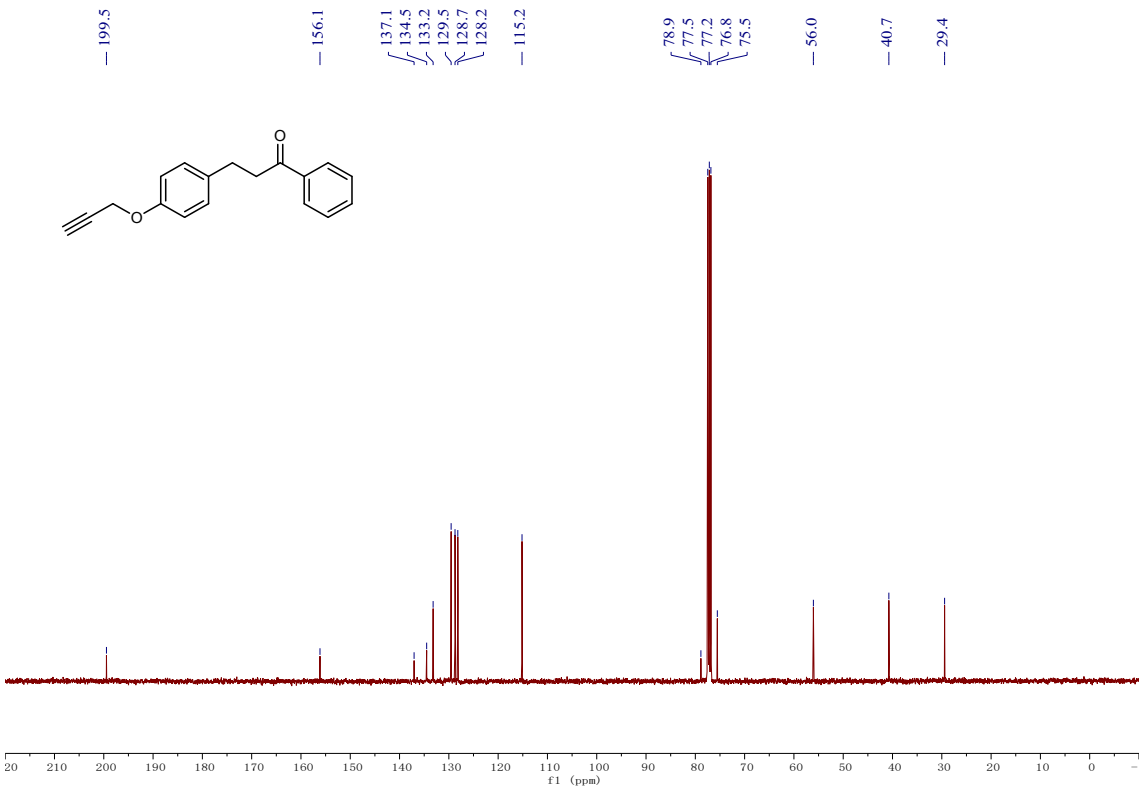

Figure S17. ^{13}C NMR (101 MHz, $CDCl_3$) spectrum of compound 2e.

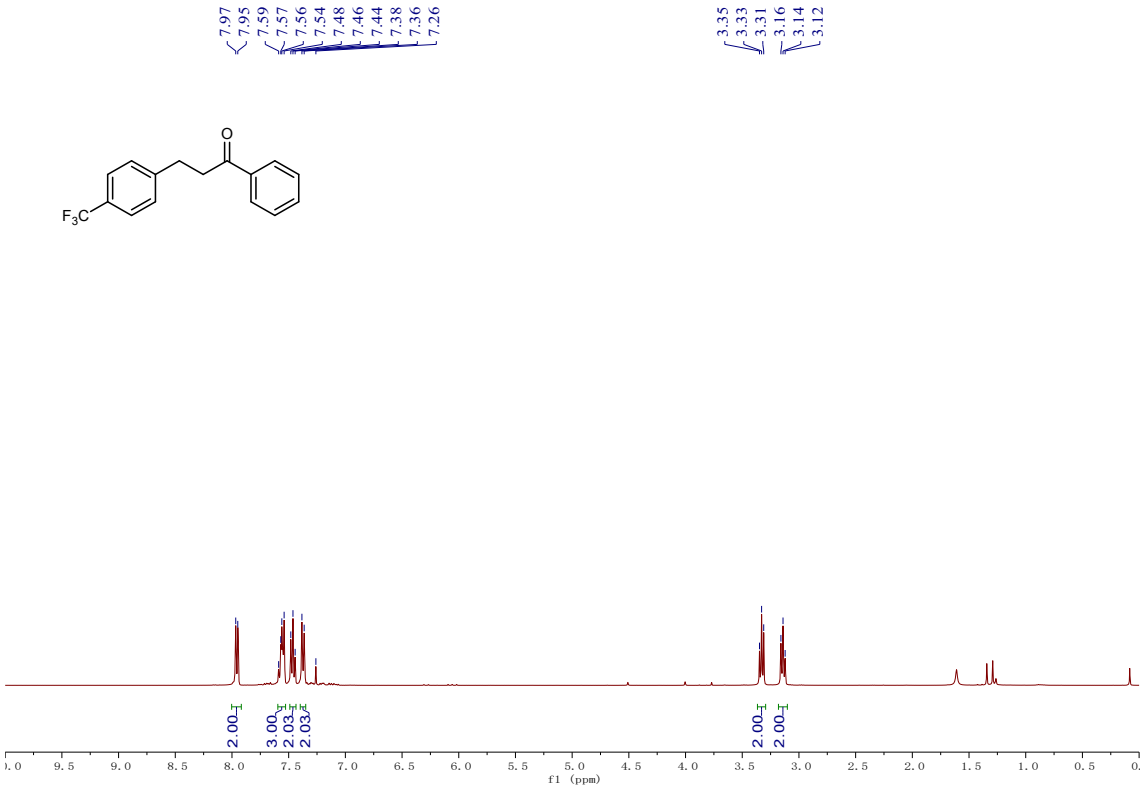

Figure S18. ^{1}H NMR (400 MHz, $CDCl_3$) spectrum of compound 2f.

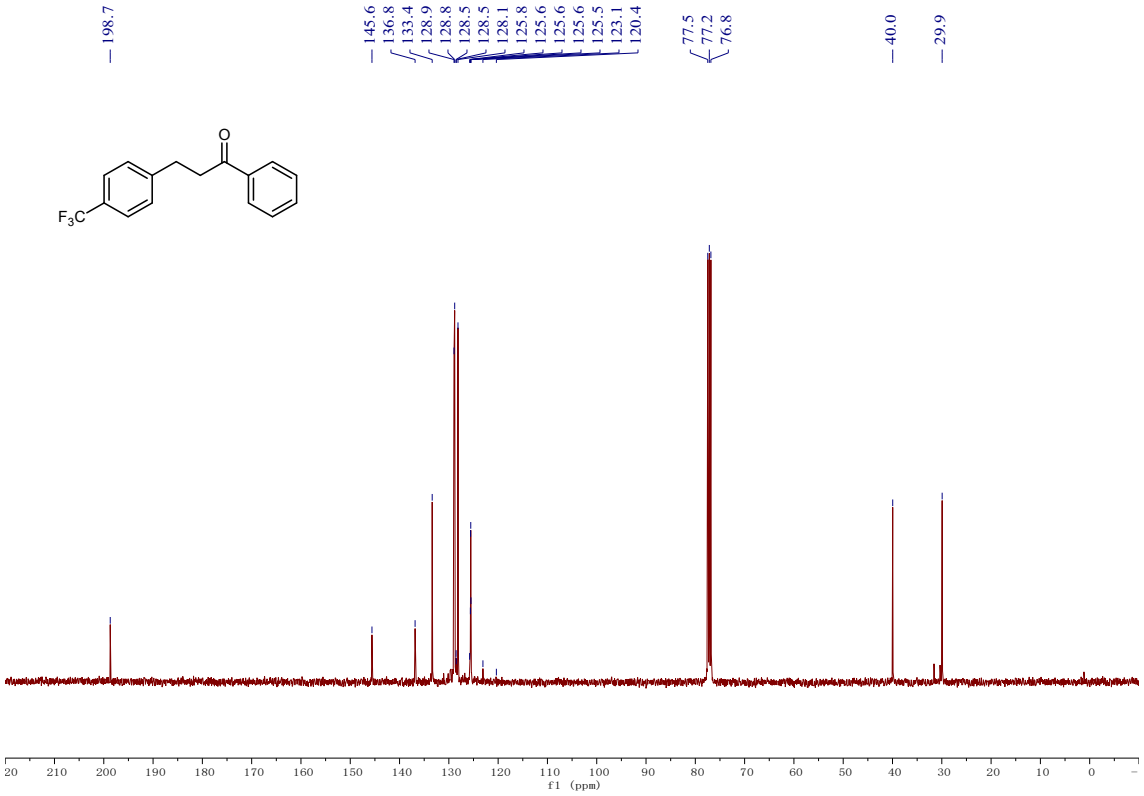

Figure S19. ^{13}C NMR (101 MHz, $CDCl_3$) spectrum of compound 2f.

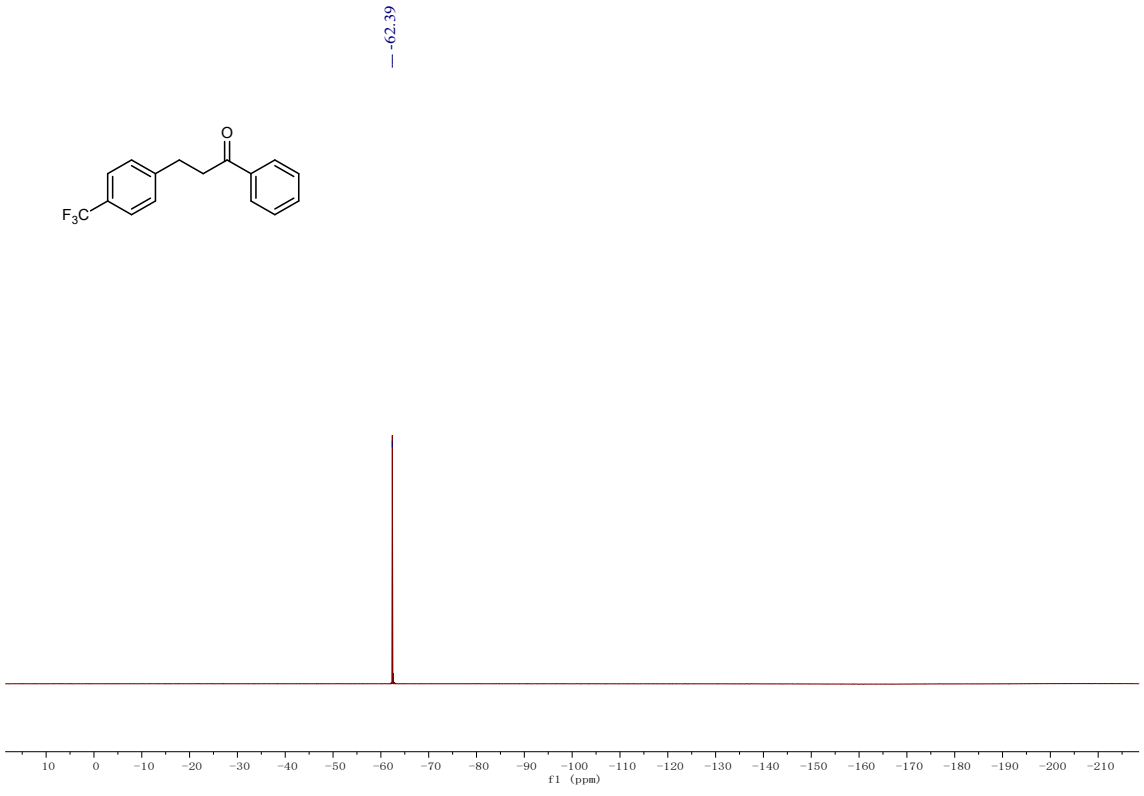

Figure S20. ^{19}F NMR (376 MHz, $CDCl_3$) spectrum of compound 2f.

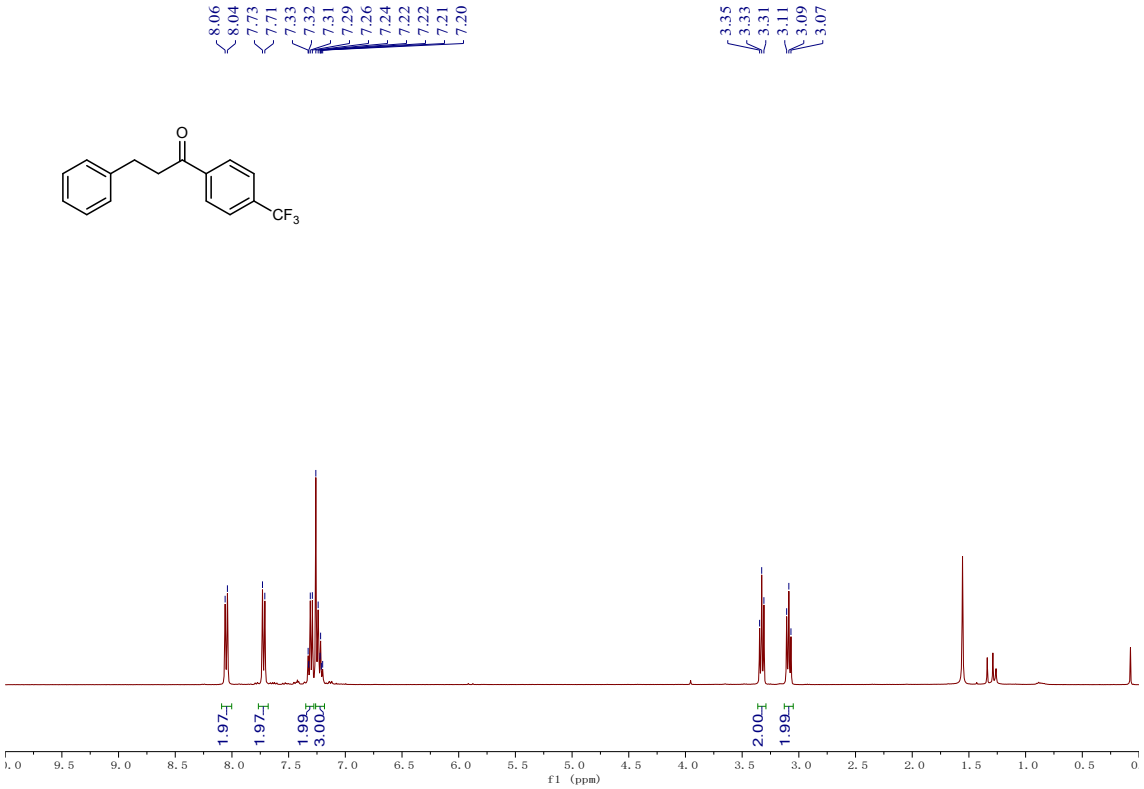

Figure S21. ^{1}H NMR (400 MHz, $CDCl_3$) spectrum of compound 2g.

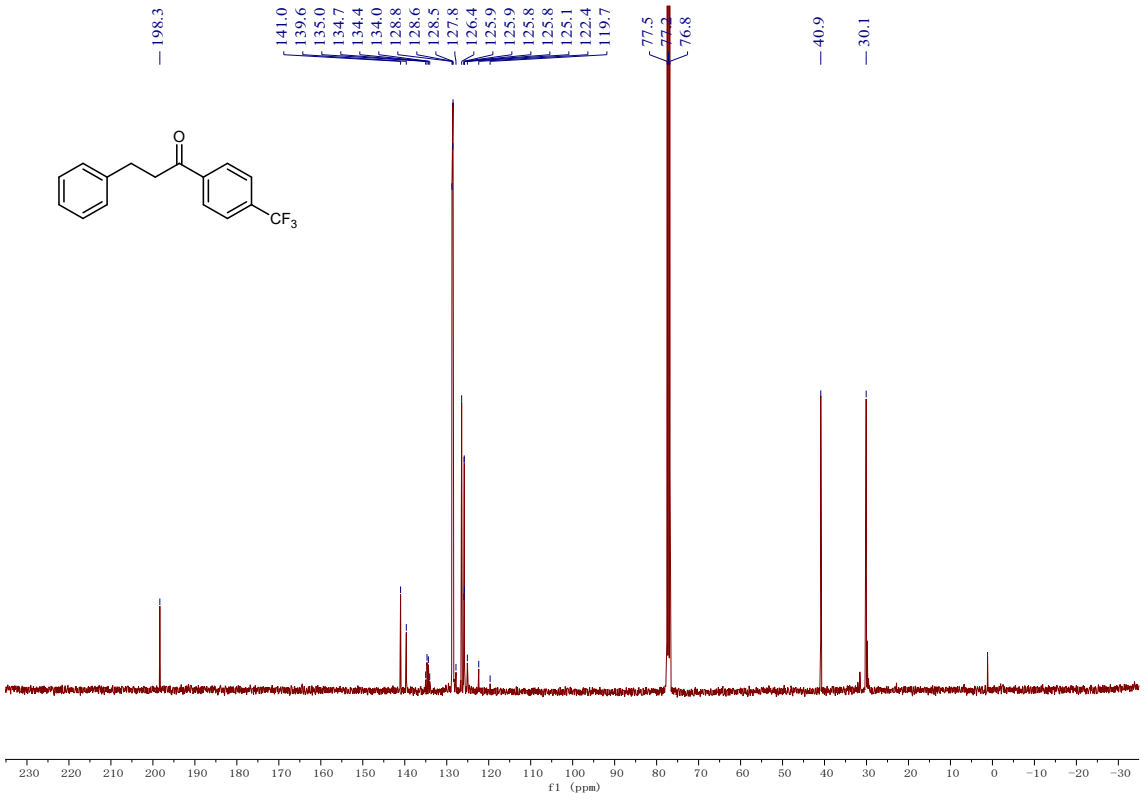

Figure S22. ^{13}C NMR (101 MHz, $CDCl_3$) spectrum of compound 2g.

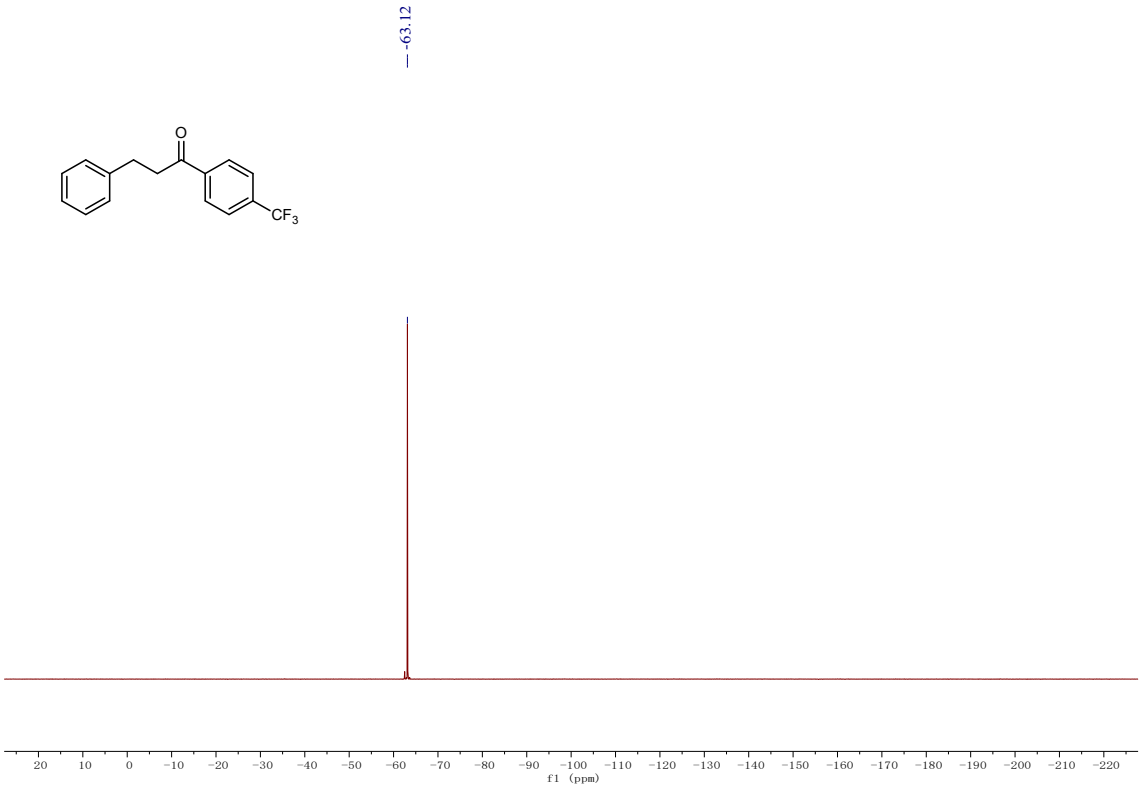

Figure S23. ^{19}F NMR (376 MHz, $CDCl_3$) spectrum of compound 2g.

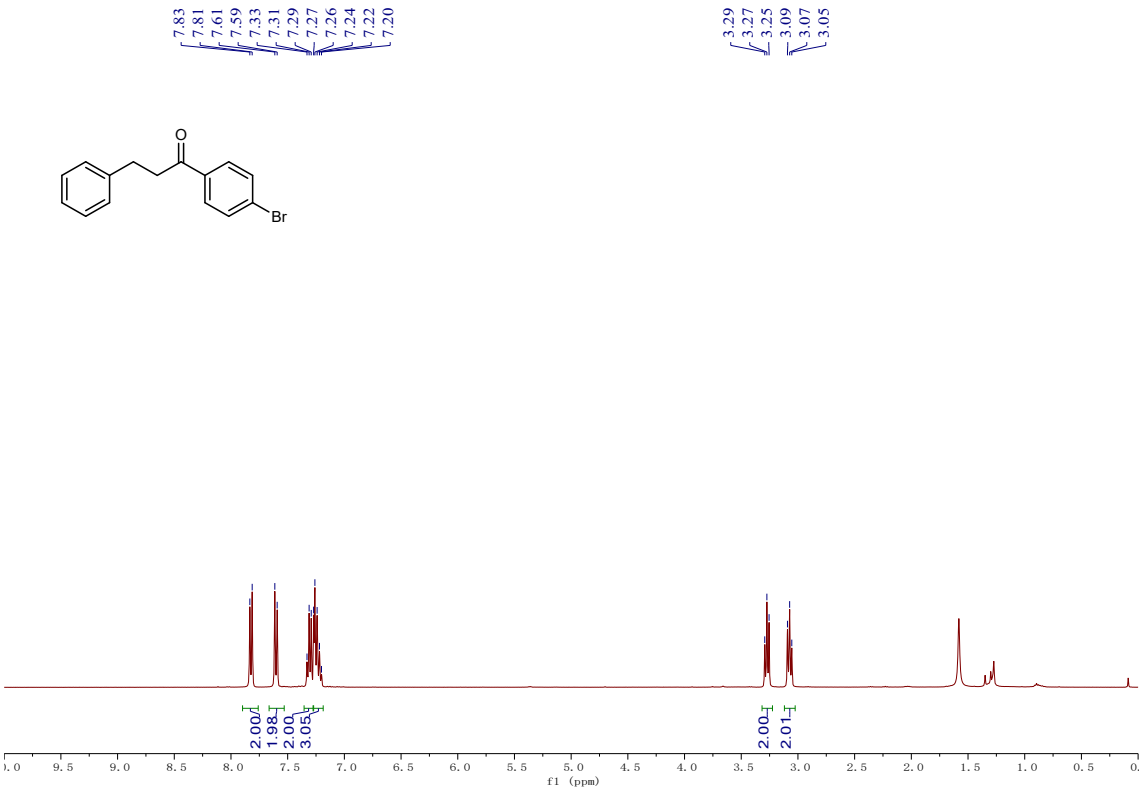

Figure S24. ^{1}H NMR (400 MHz, $CDCl_3$) spectrum of compound 2h.

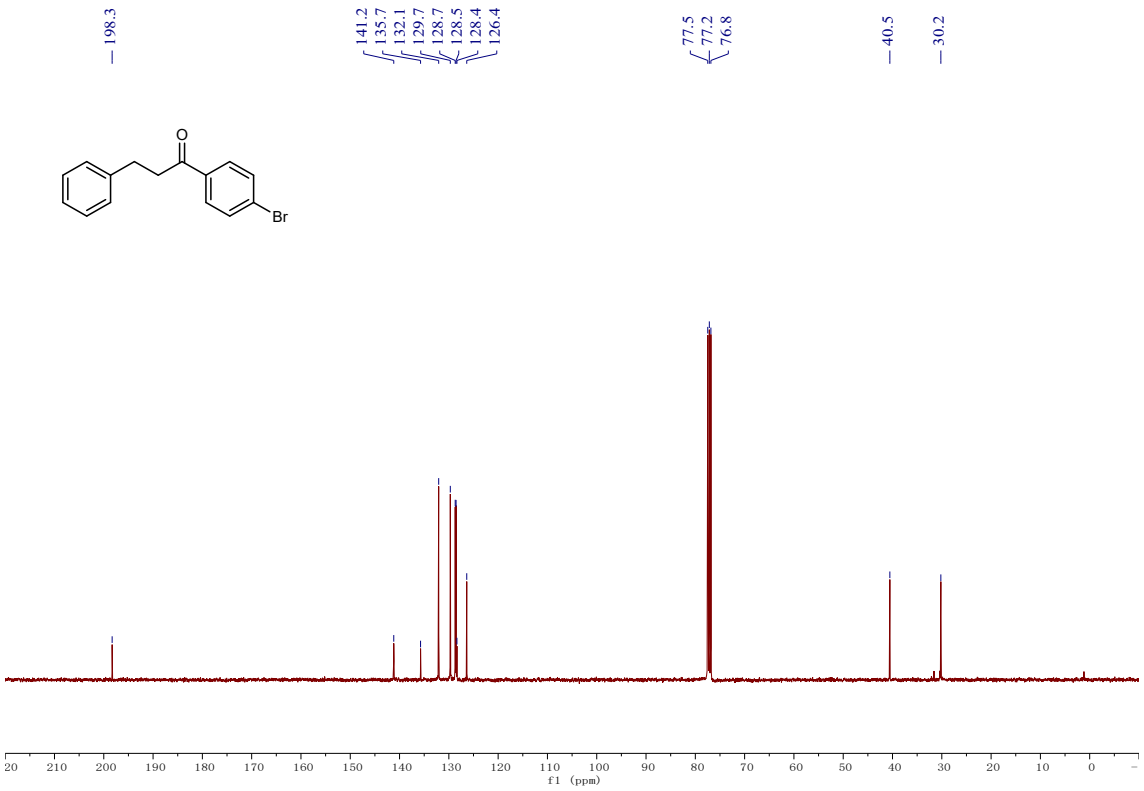

Figure S25. ^{13}C NMR (101 MHz, $CDCl_3$) spectrum of compound 2h.

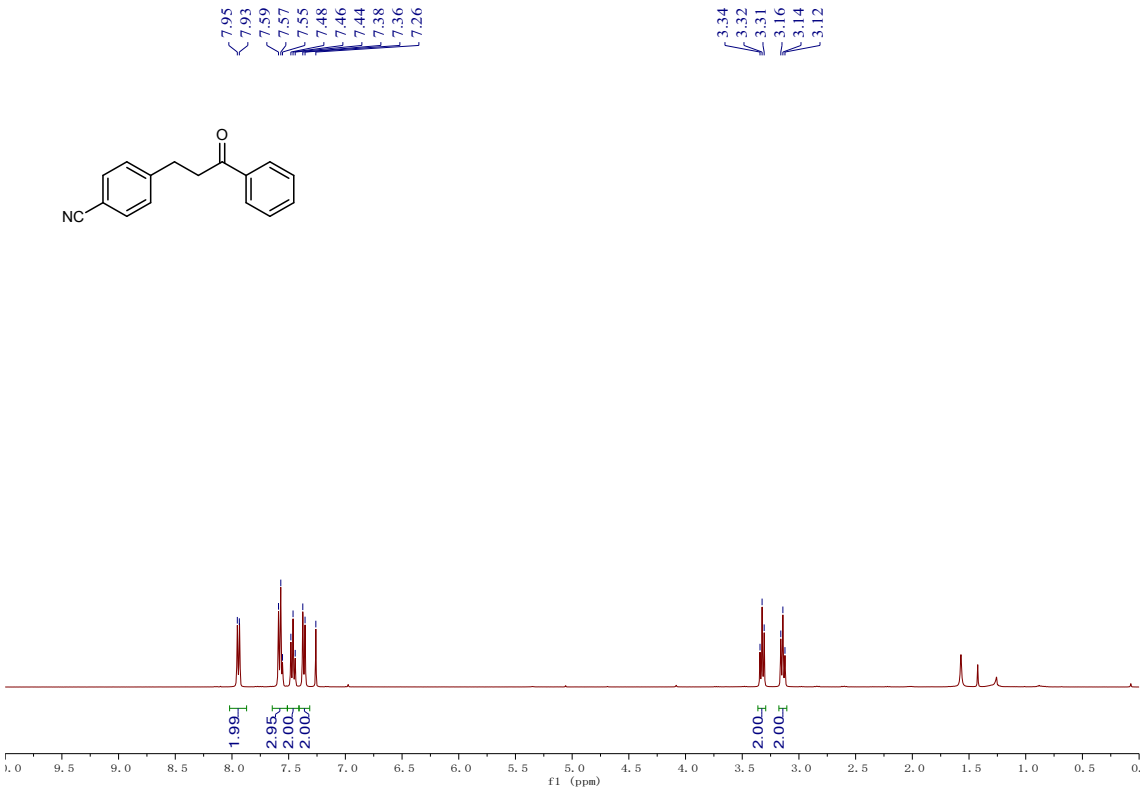

Figure S26. ^{1}H NMR (400 MHz, $CDCl_3$) spectrum of compound 2i.

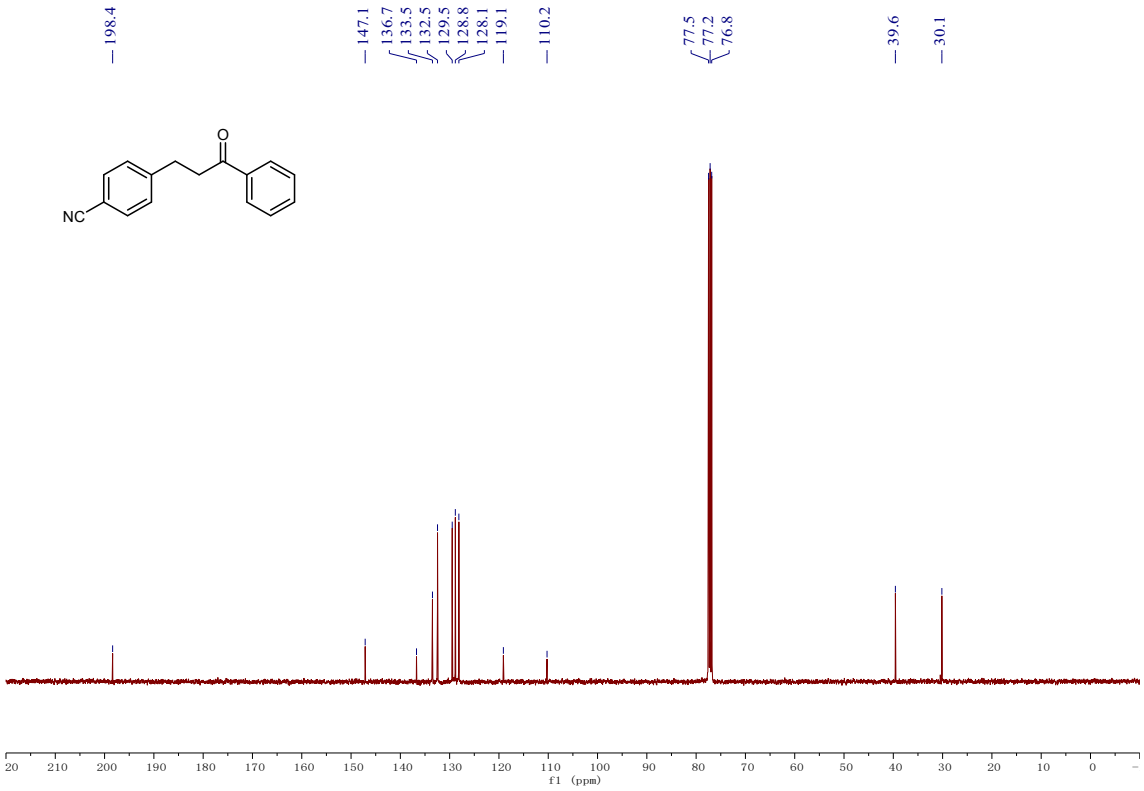

Figure S27. ^{13}C NMR (101 MHz, $CDCl_3$) spectrum of compound 2i.

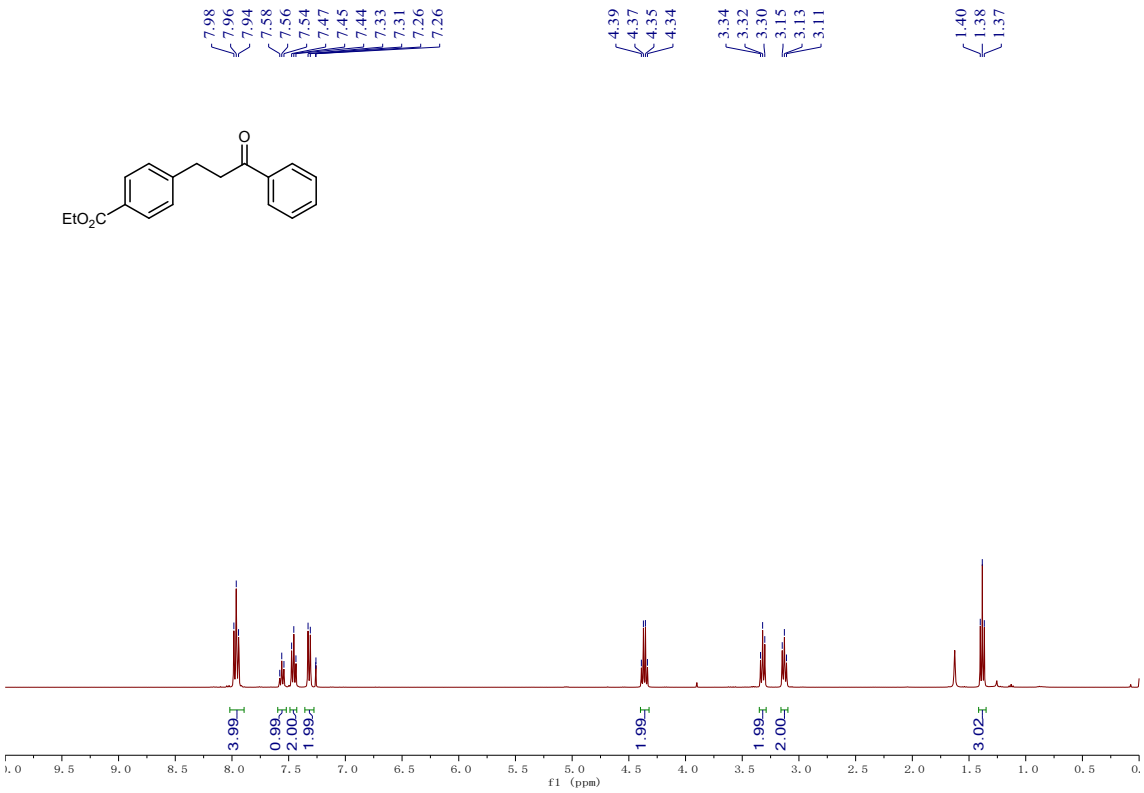

Figure S28. ^{1}H NMR (400 MHz, $CDCl_3$) spectrum of compound 2j.

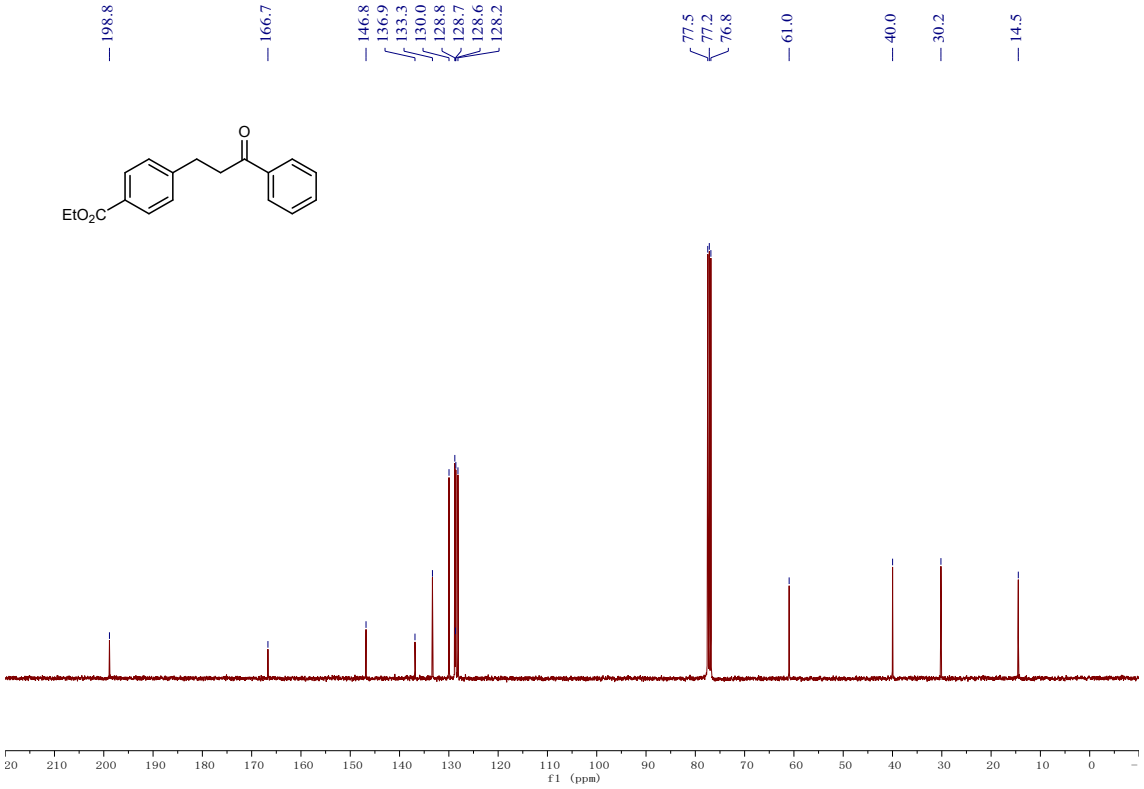

Figure S29. ^{13}C NMR (101 MHz, $CDCl_3$) spectrum of compound 2j.

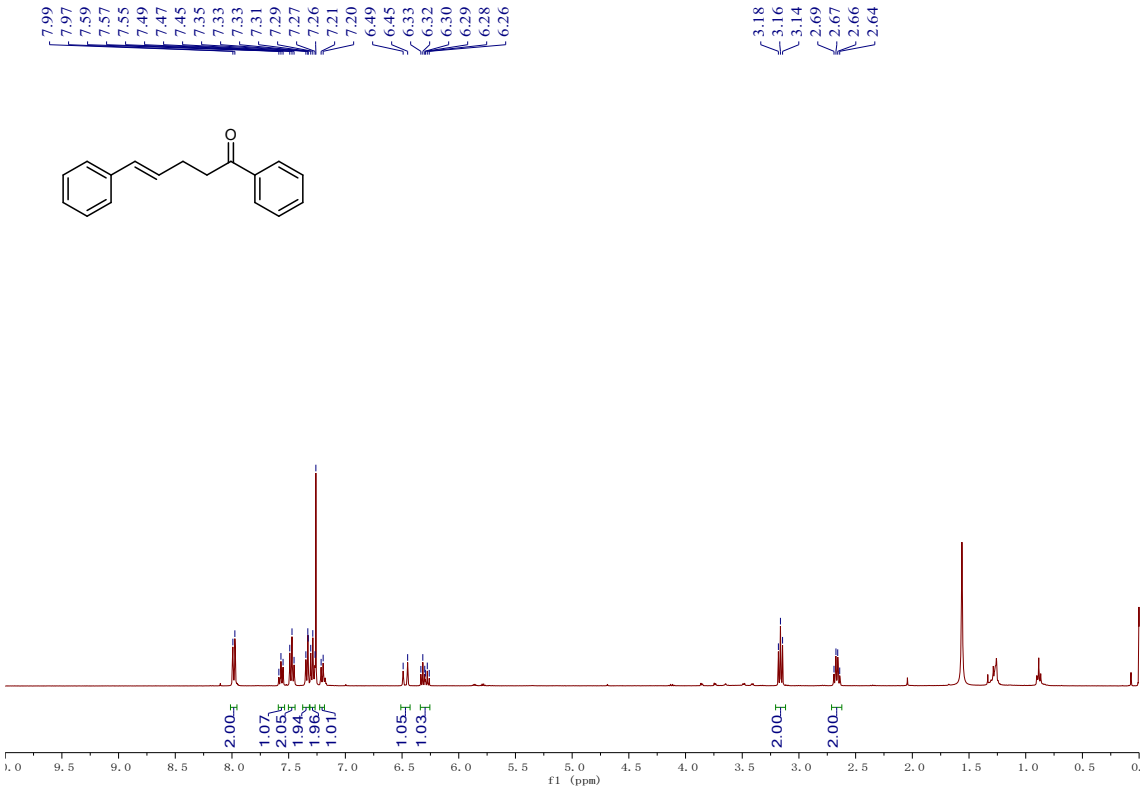

Figure S30. ^{1}H NMR (400 MHz, $CDCl_3$) spectrum of compound 2k.

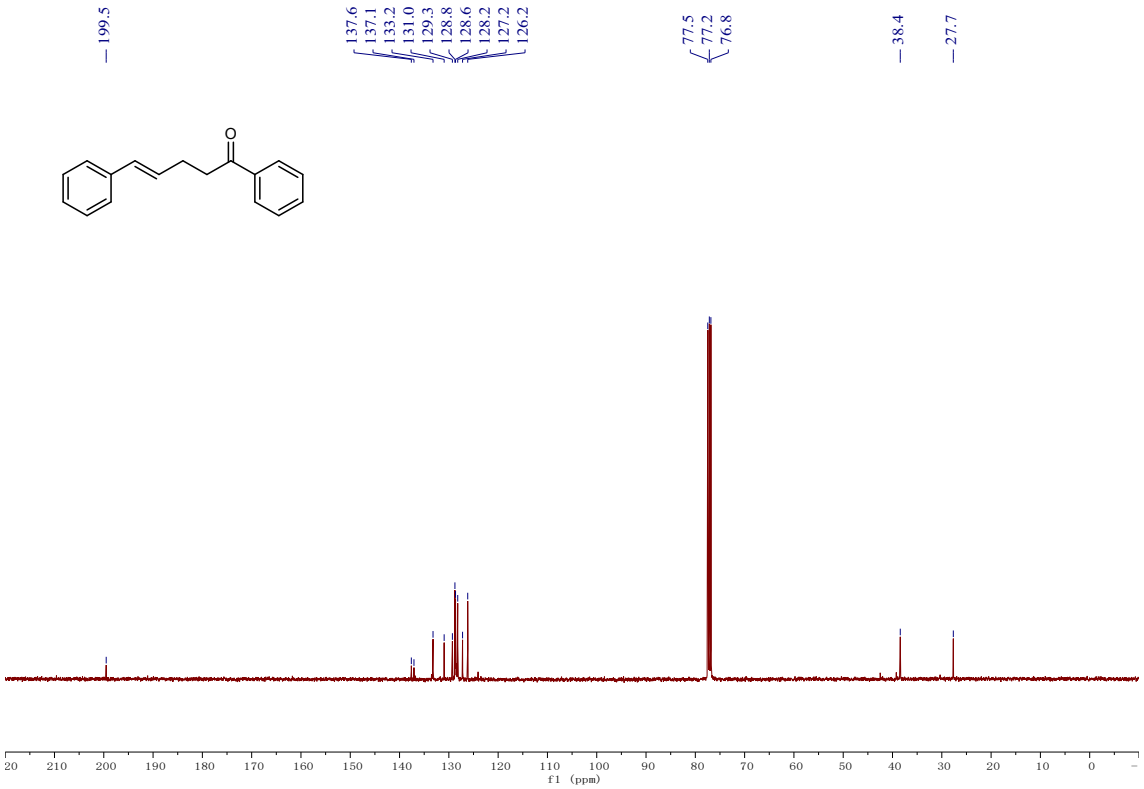

Figure S31. ^{13}C NMR (101 MHz, $CDCl_3$) spectrum of compound 2k.

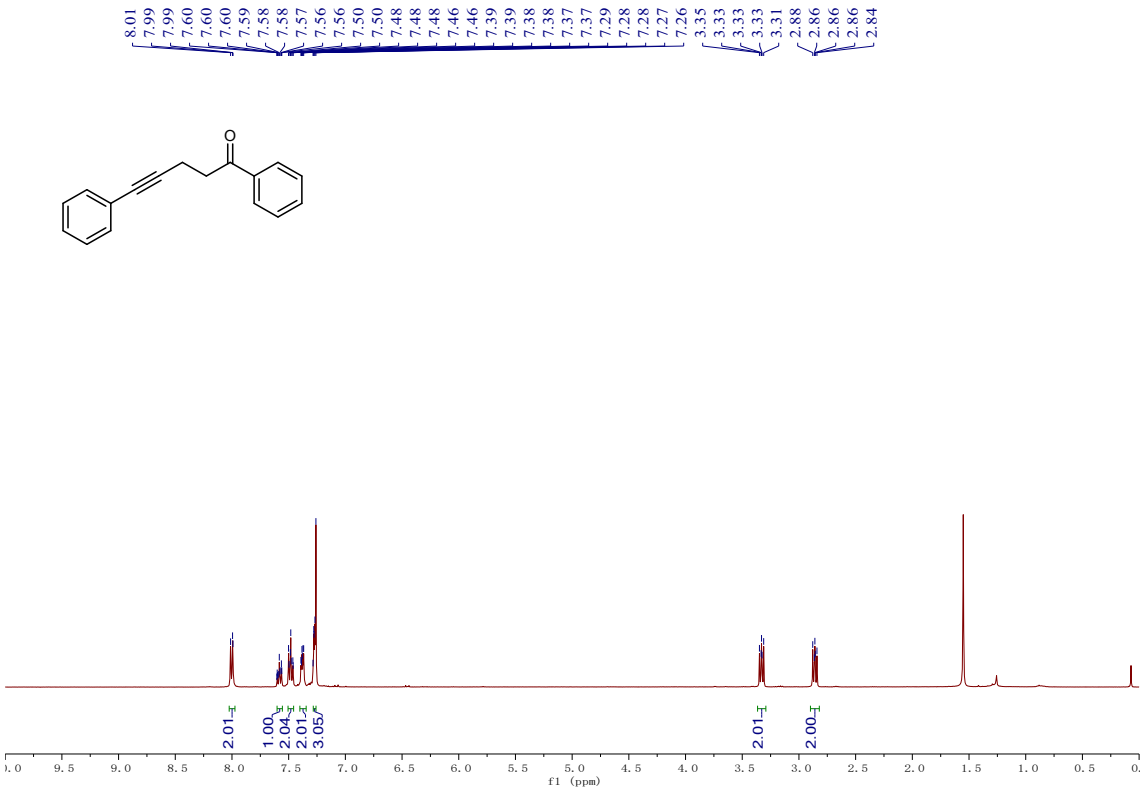

Figure S32. ^{1}H NMR (400 MHz, $CDCl_3$) spectrum of compound 2l.

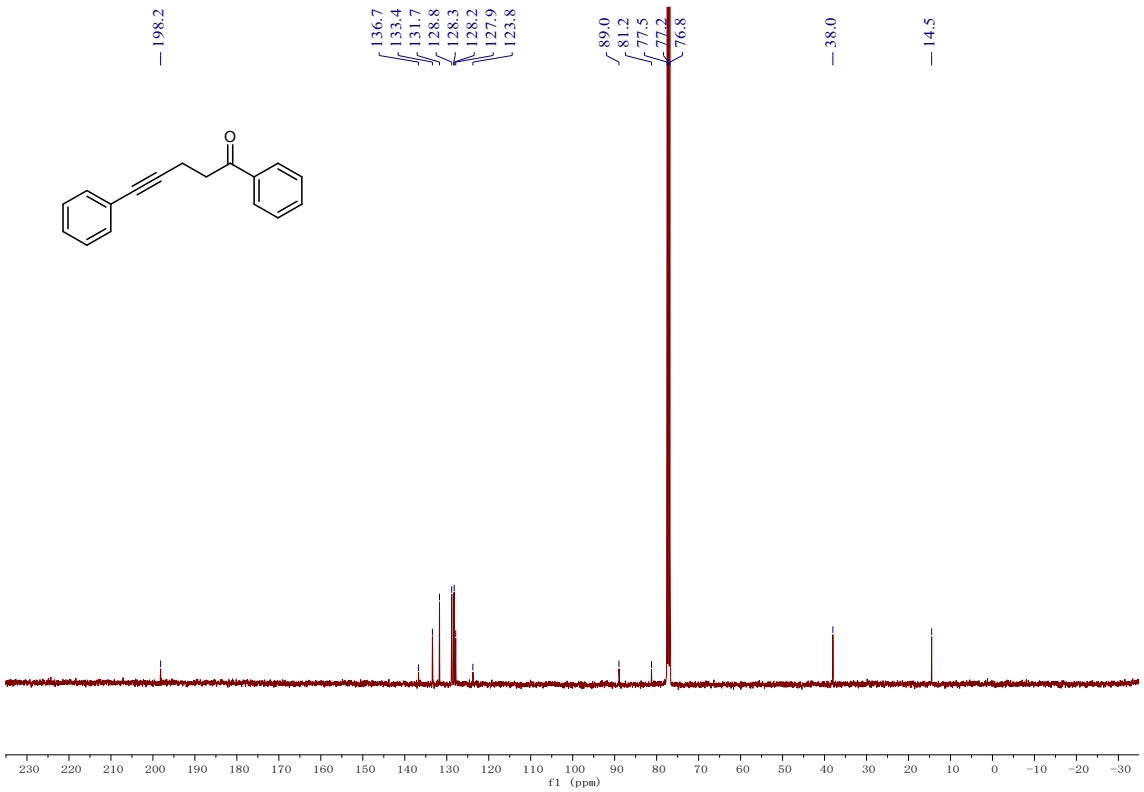

Figure S33. ^{13}C NMR (101 MHz, $CDCl_3$) spectrum of compound 2l.

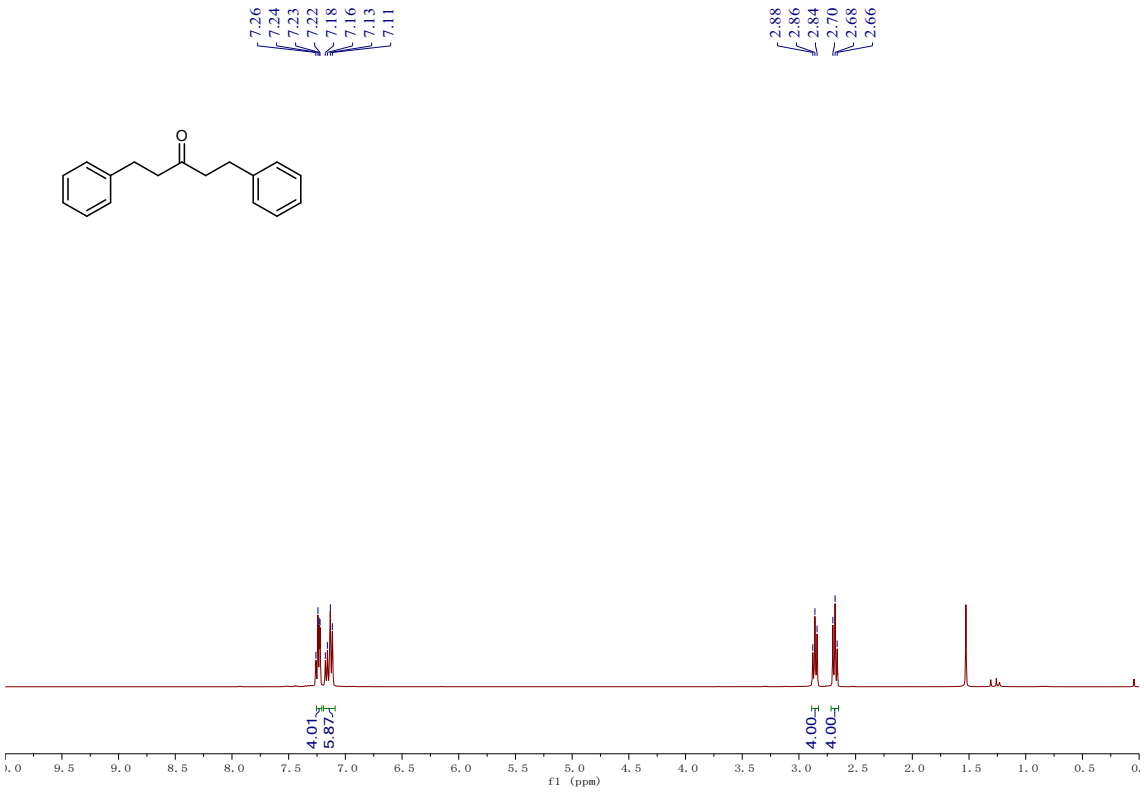

Figure S34. ^{1}H NMR (400 MHz, $CDCl_3$) spectrum of compound 2m.

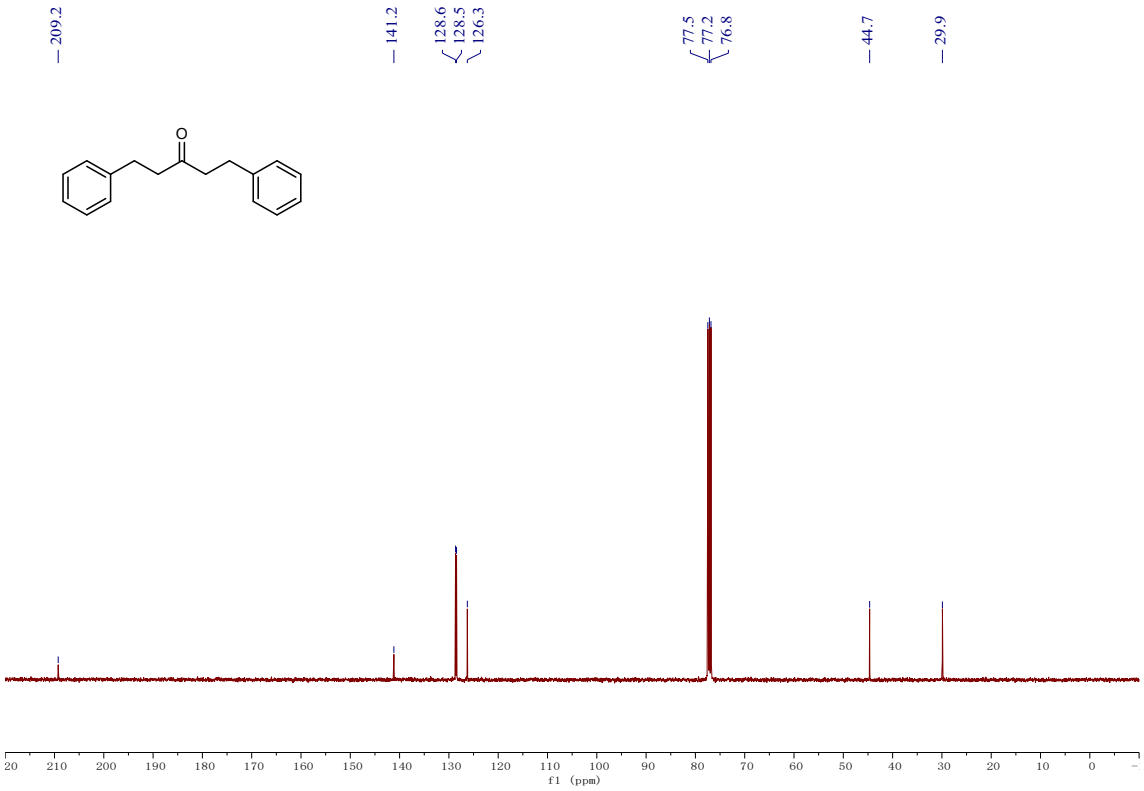

Figure S35. ^{13}C NMR (101 MHz, $CDCl_3$) spectrum of compound 2m.

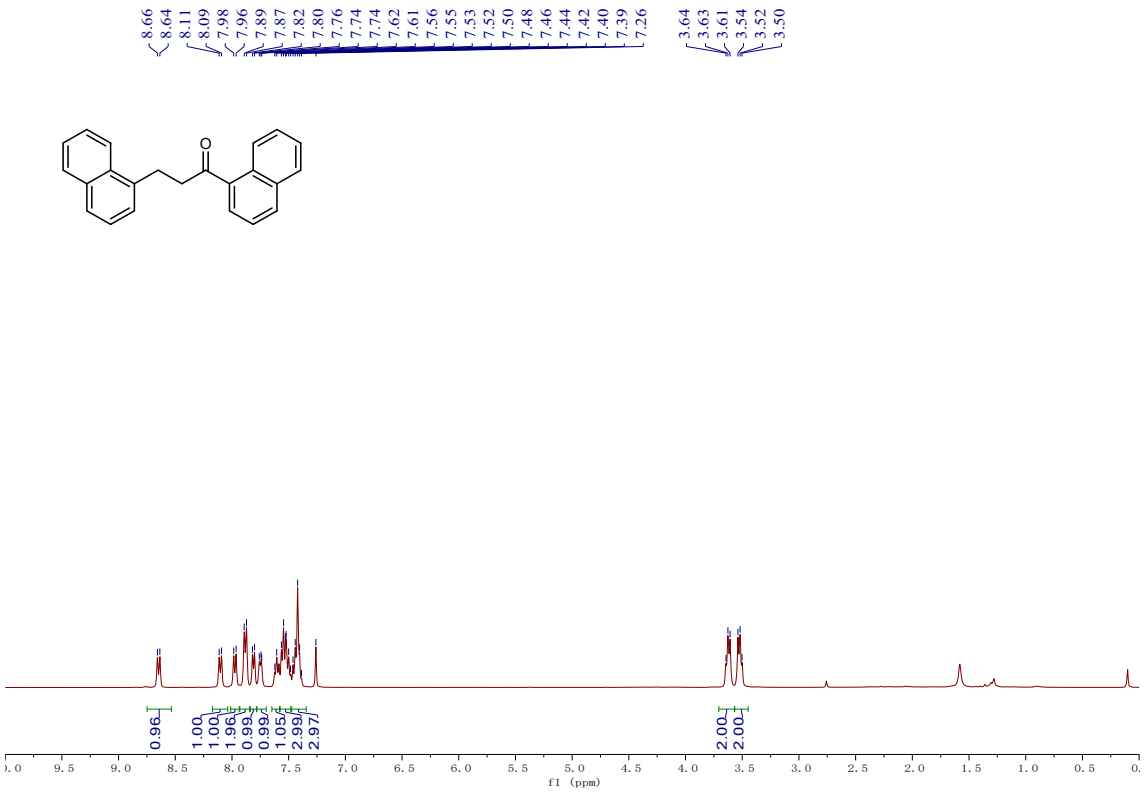

Figure S36. ^{1}H NMR (400 MHz, CDCl3) spectrum of compound 2n.

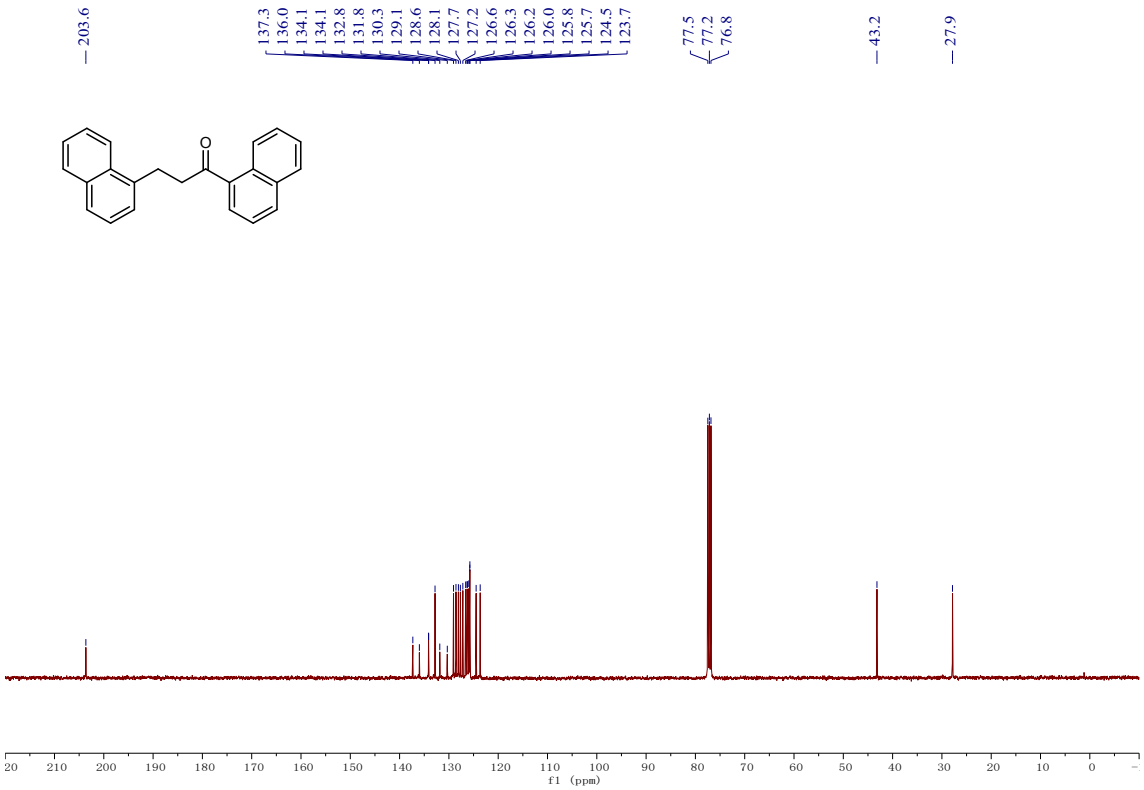

Figure S37. ^{13}C NMR (101 MHz, $CDCl_3$) spectrum of compound 2n.

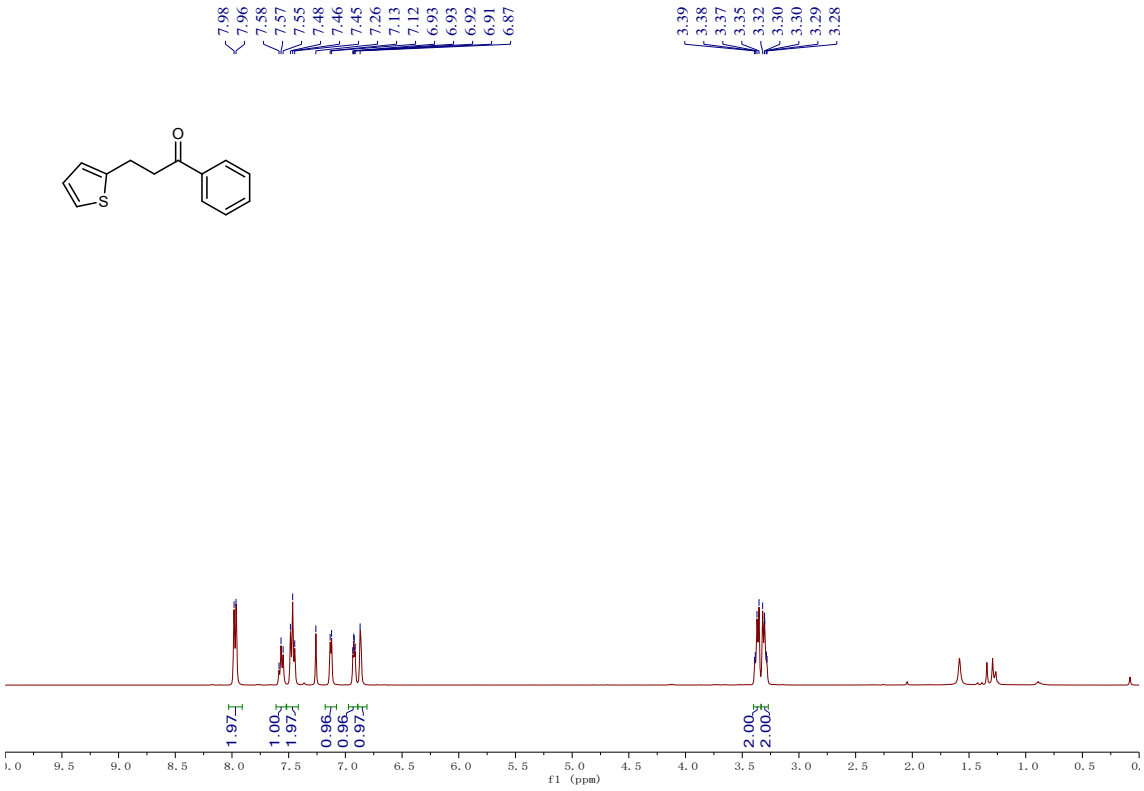

Figure S38. ^{1}H NMR (400 MHz, $CDCl_3$) spectrum of compound 2o.

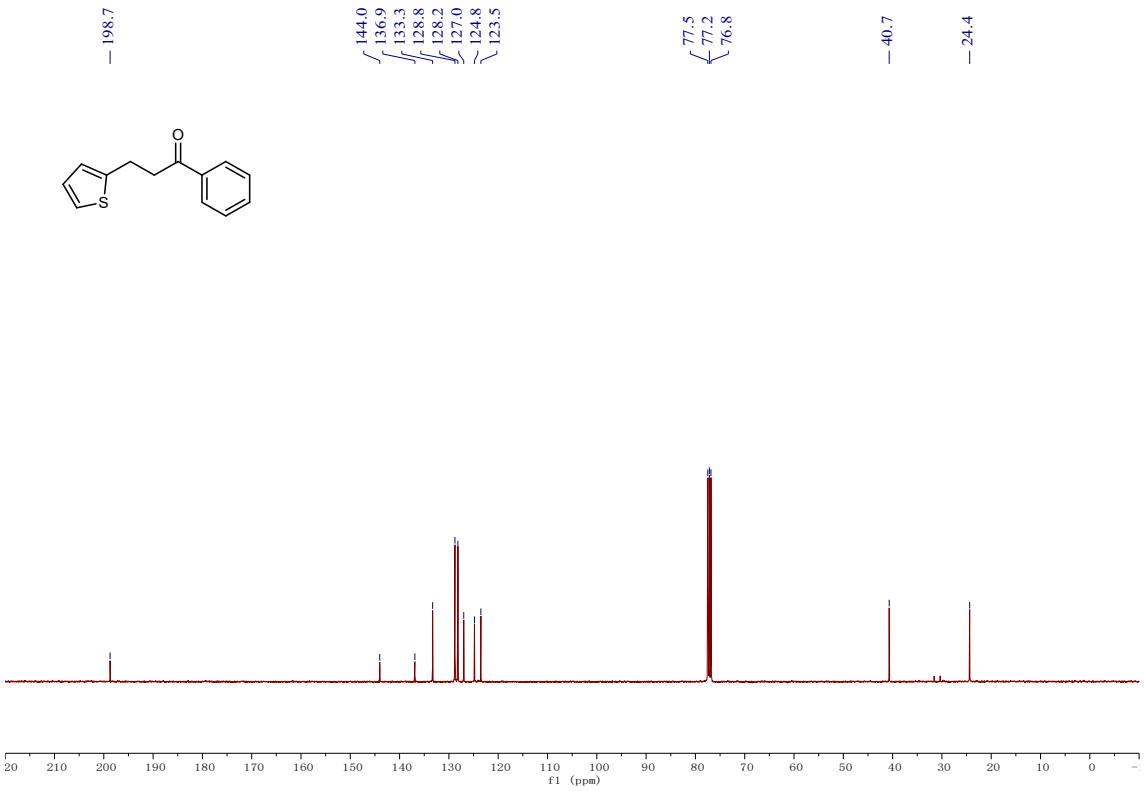

Figure S39. ^{13}C NMR (101 MHz, $CDCl_3$) spectrum of compound 2o.

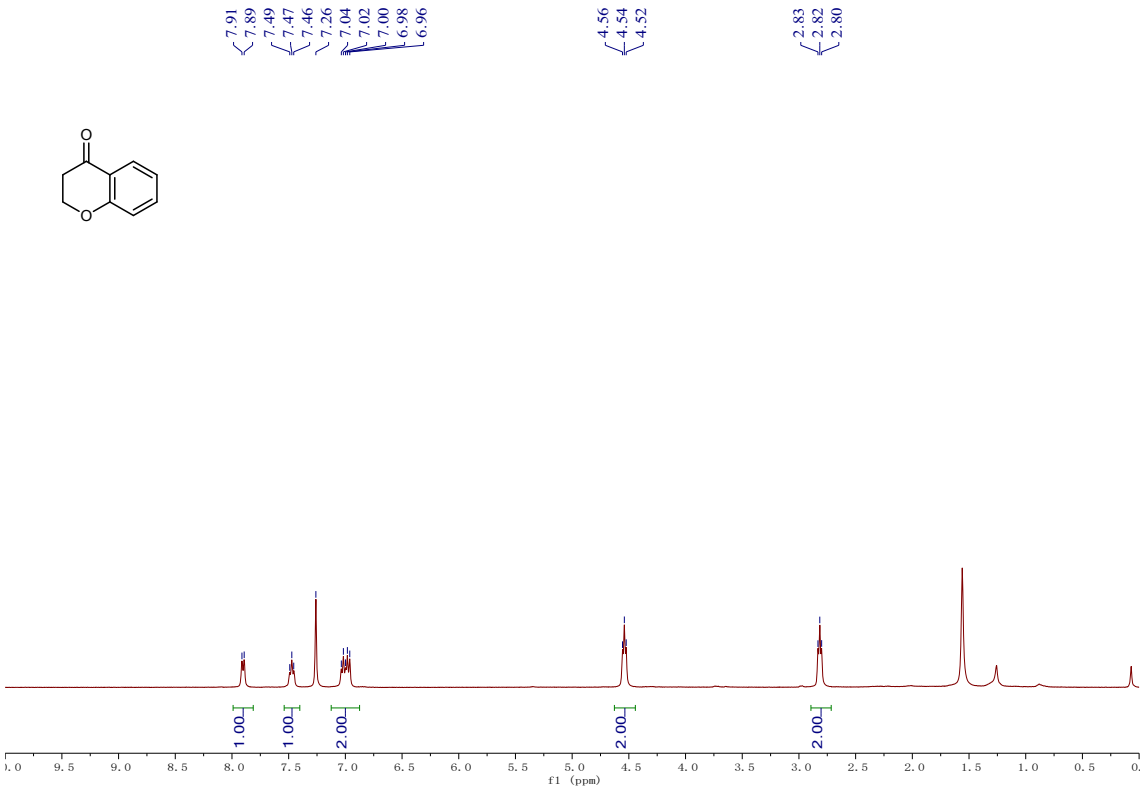

Figure S40. ^{1}H NMR (400 MHz, $CDCl_3$) spectrum of compound 2p.

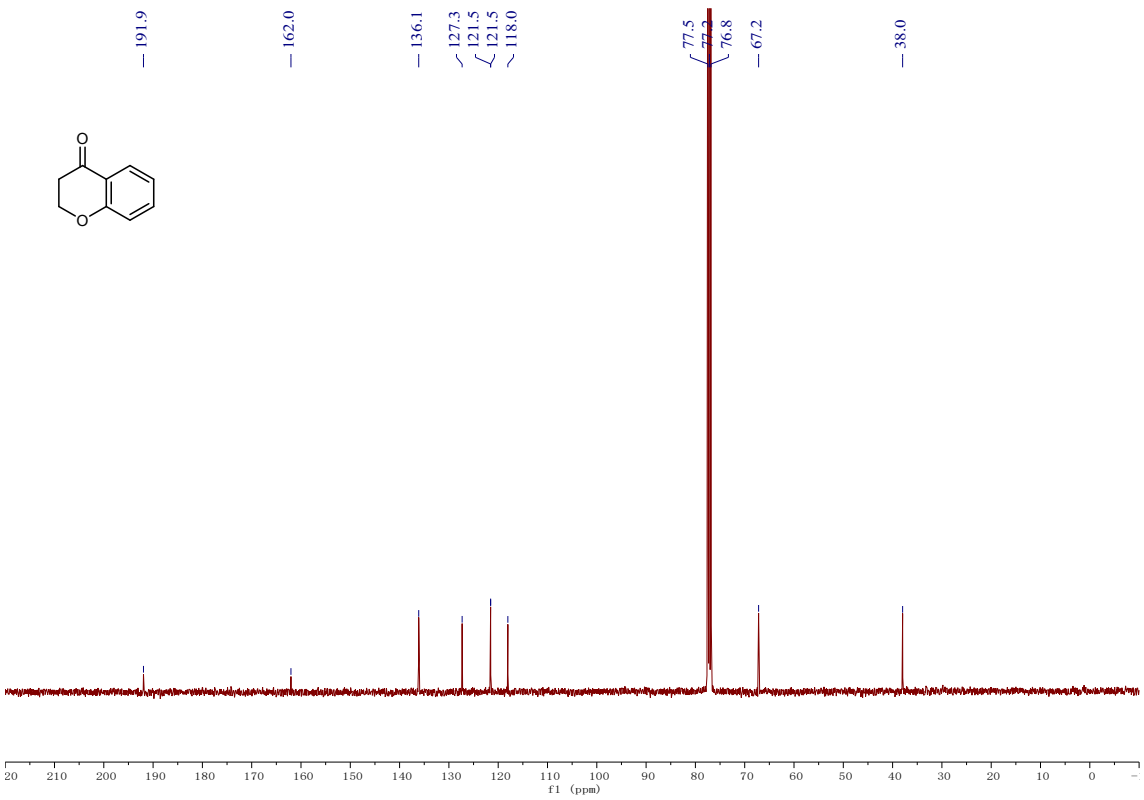

Figure S41. ^{13}C NMR (101 MHz, $CDCl_3$) spectrum of compound 2p.

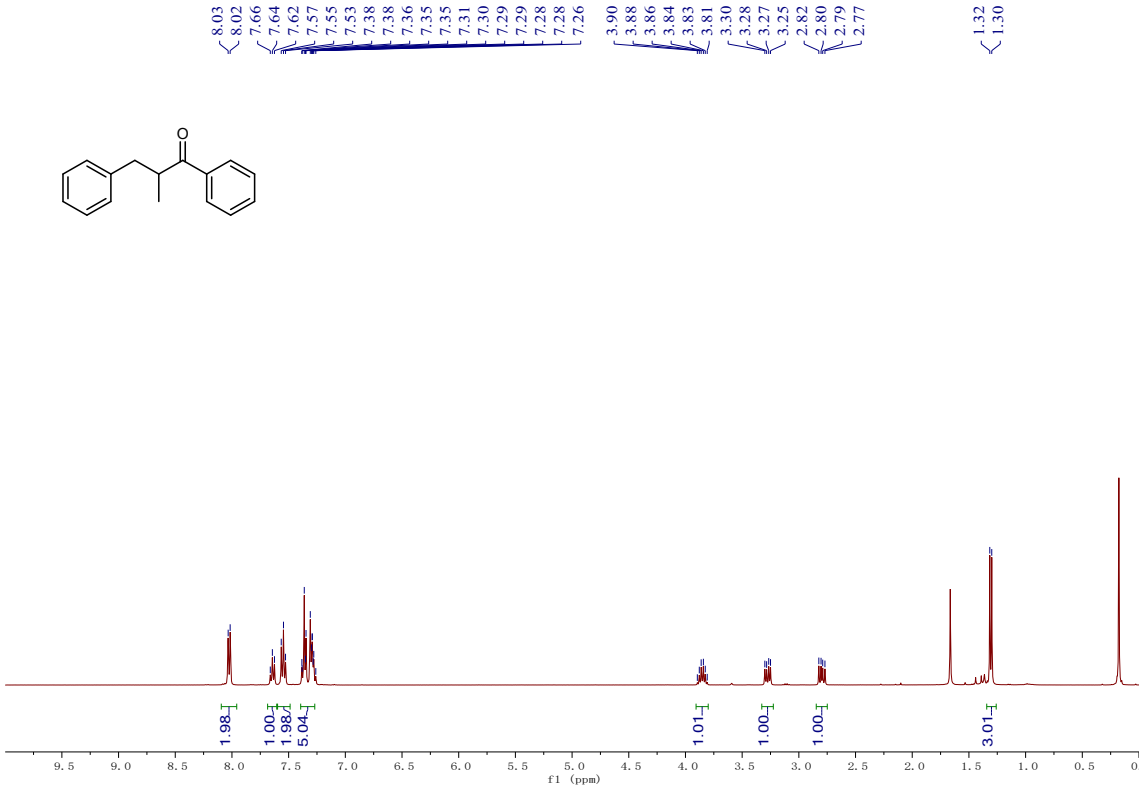

Figure S42. ^{1}H NMR (400 MHz, $CDCl_3$) spectrum of compound 2q.

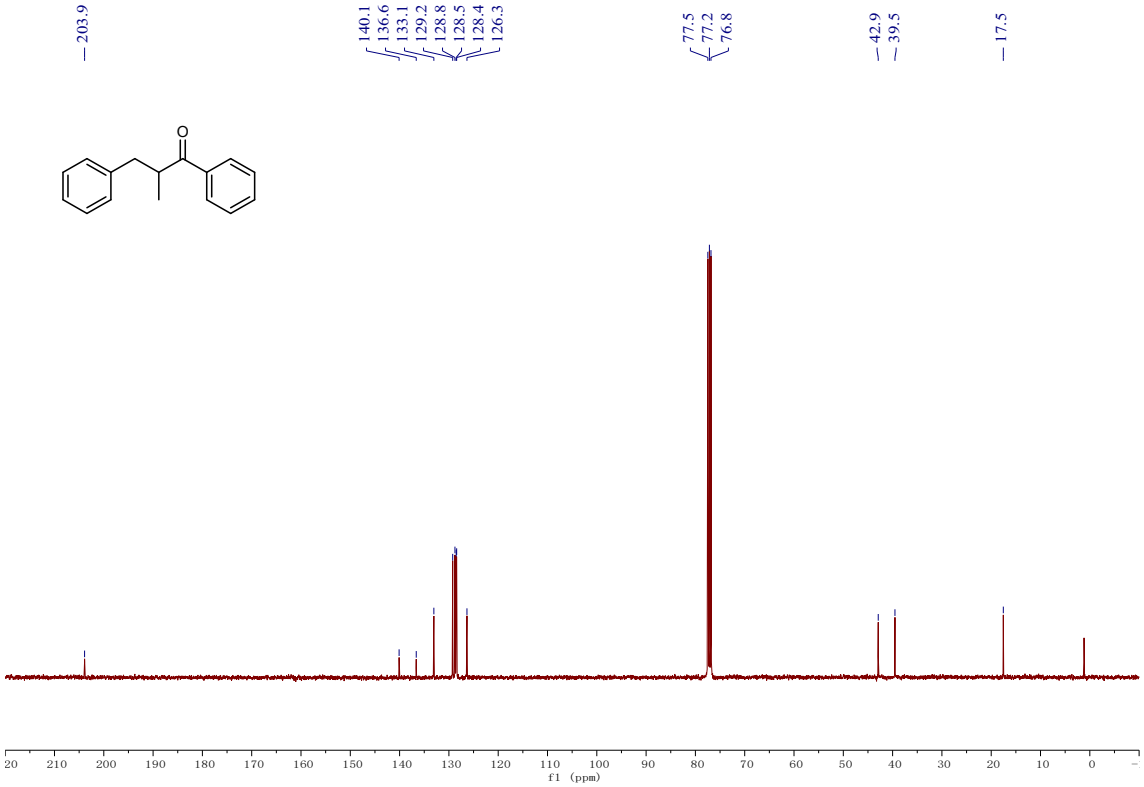

Figure S43. ^{13}C NMR (101 MHz, $CDCl_3$) spectrum of compound 2q.

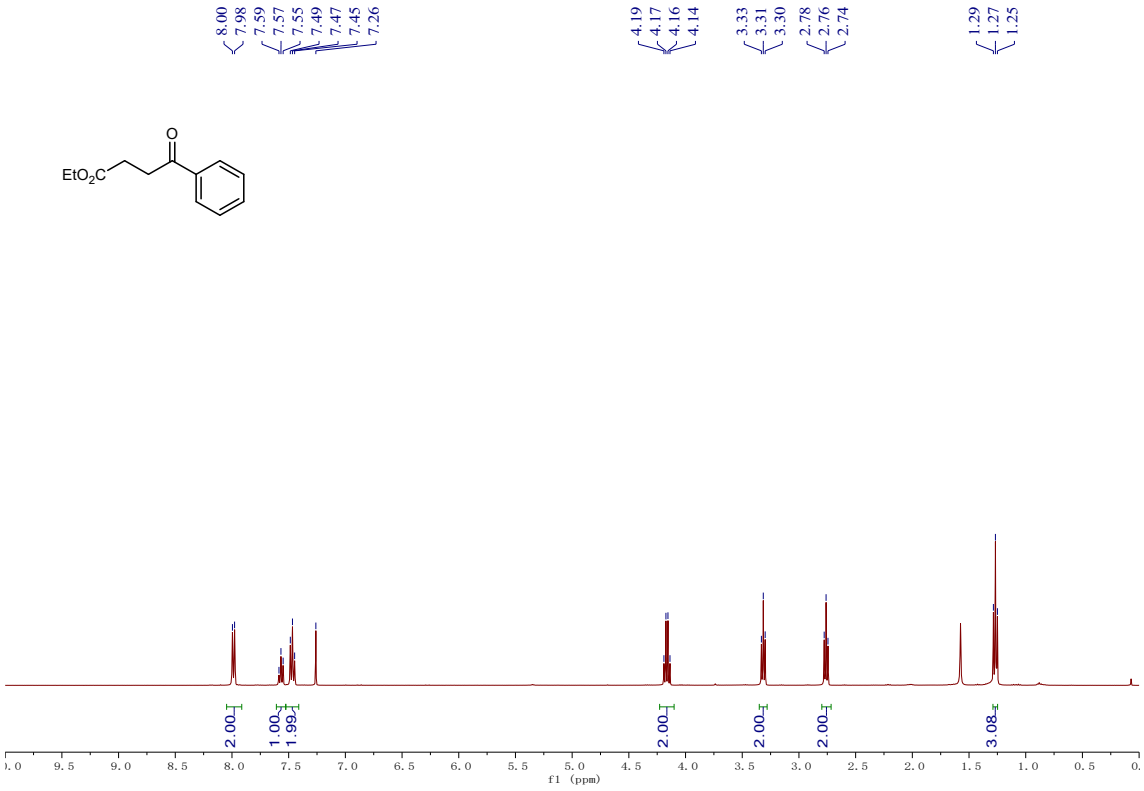

Figure S44. ^{1}H NMR (400 MHz, $CDCl_3$) spectrum of compound 2r.

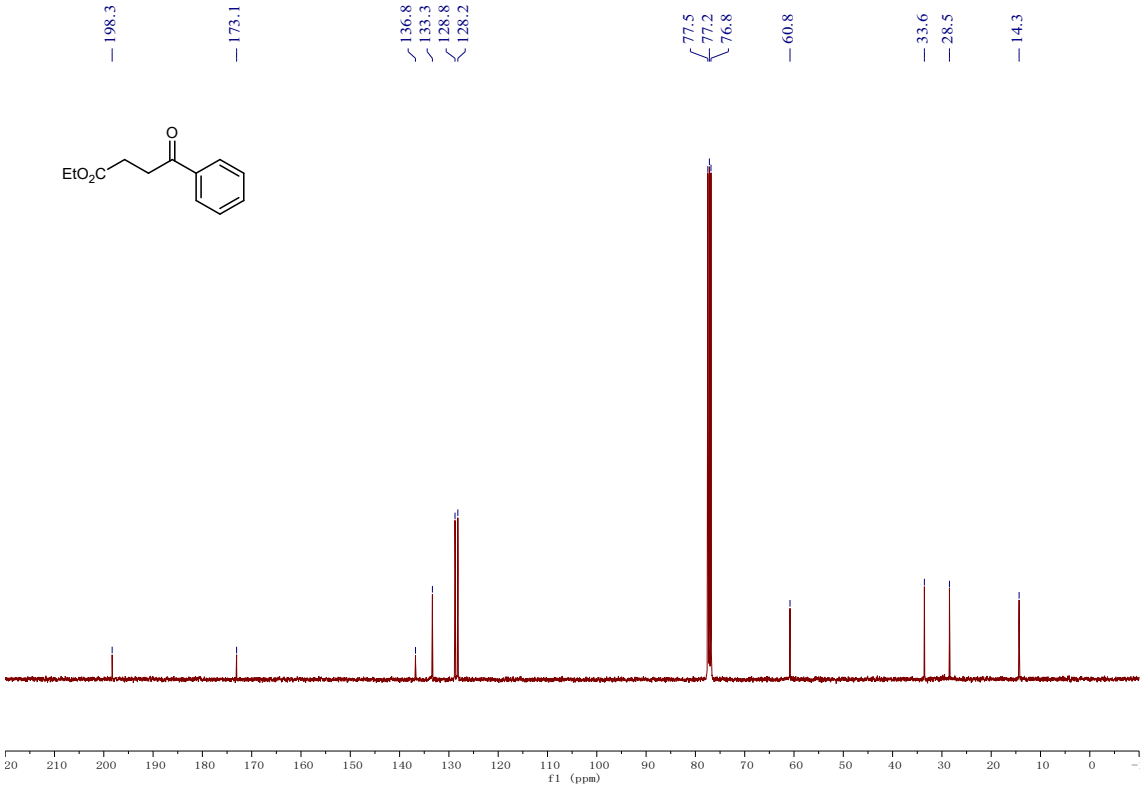

Figure S45. ^{13}C NMR (101 MHz, $CDCl_3$) spectrum of compound 2r.

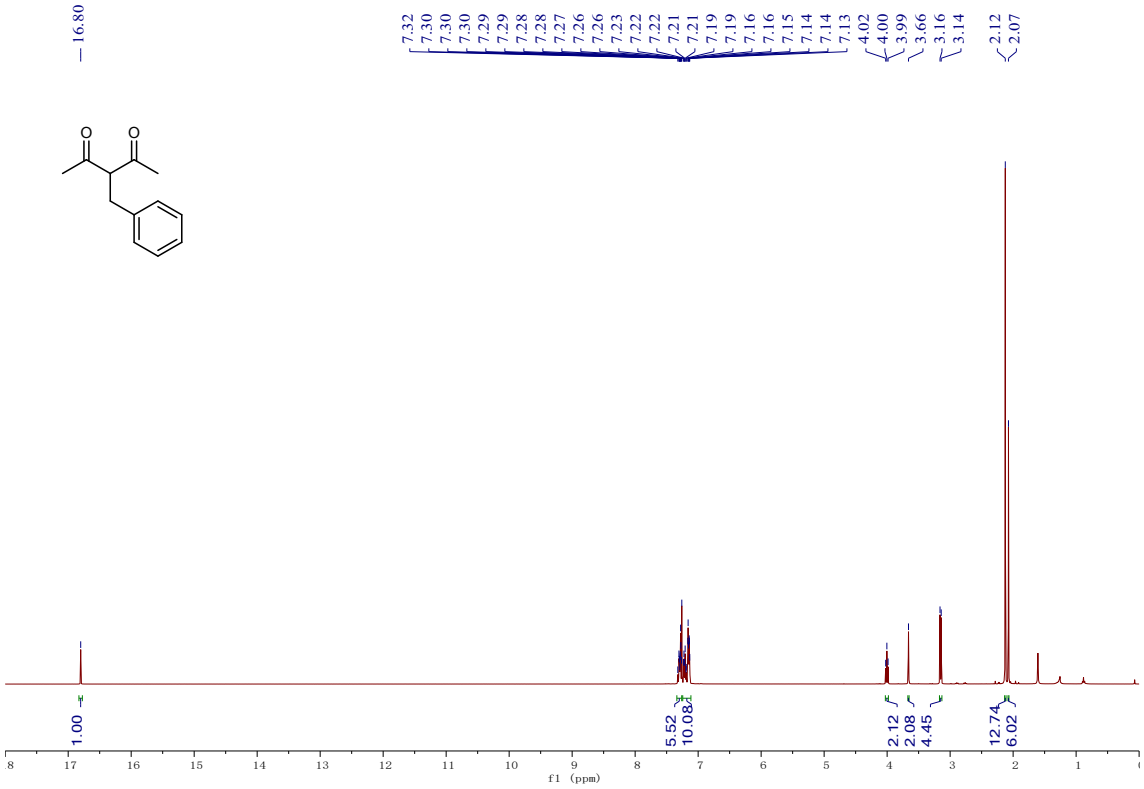

Figure S46. ^{1}H NMR (400 MHz, $CDCl_3$) spectrum of compound 2s.

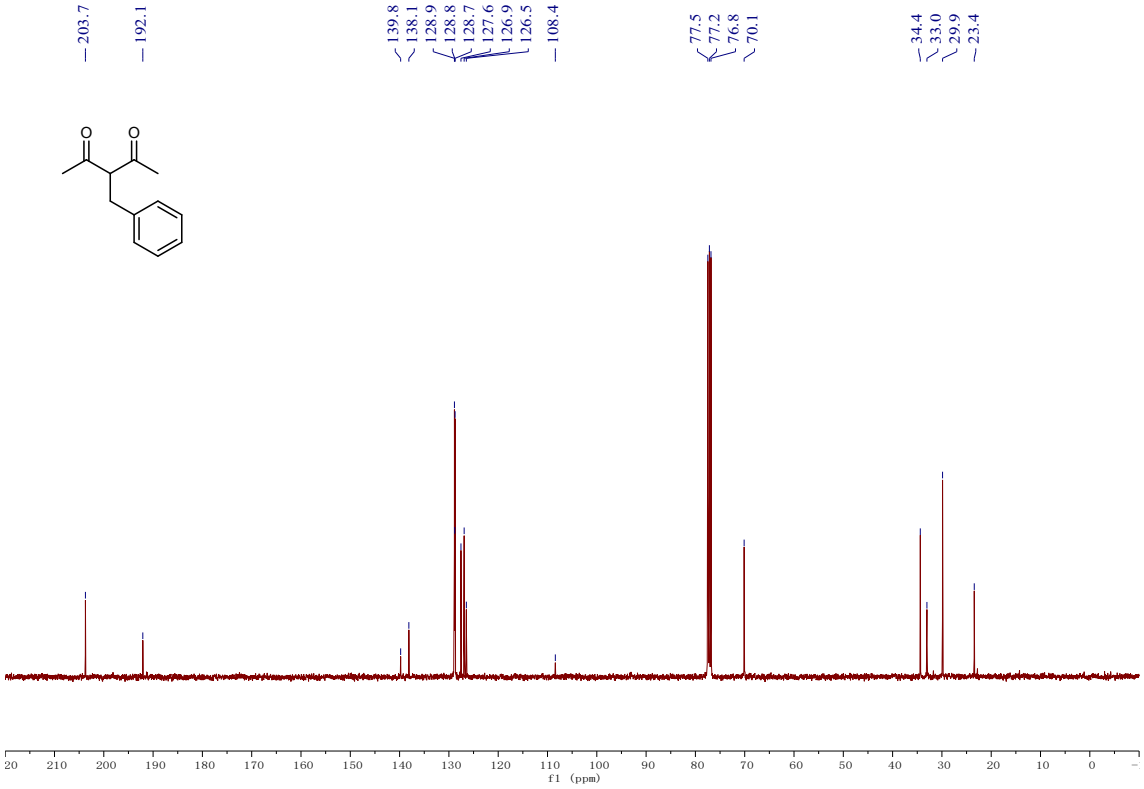

Figure S47. ^{13}C NMR (101 MHz, $CDCl_3$) spectrum of compound 2s.

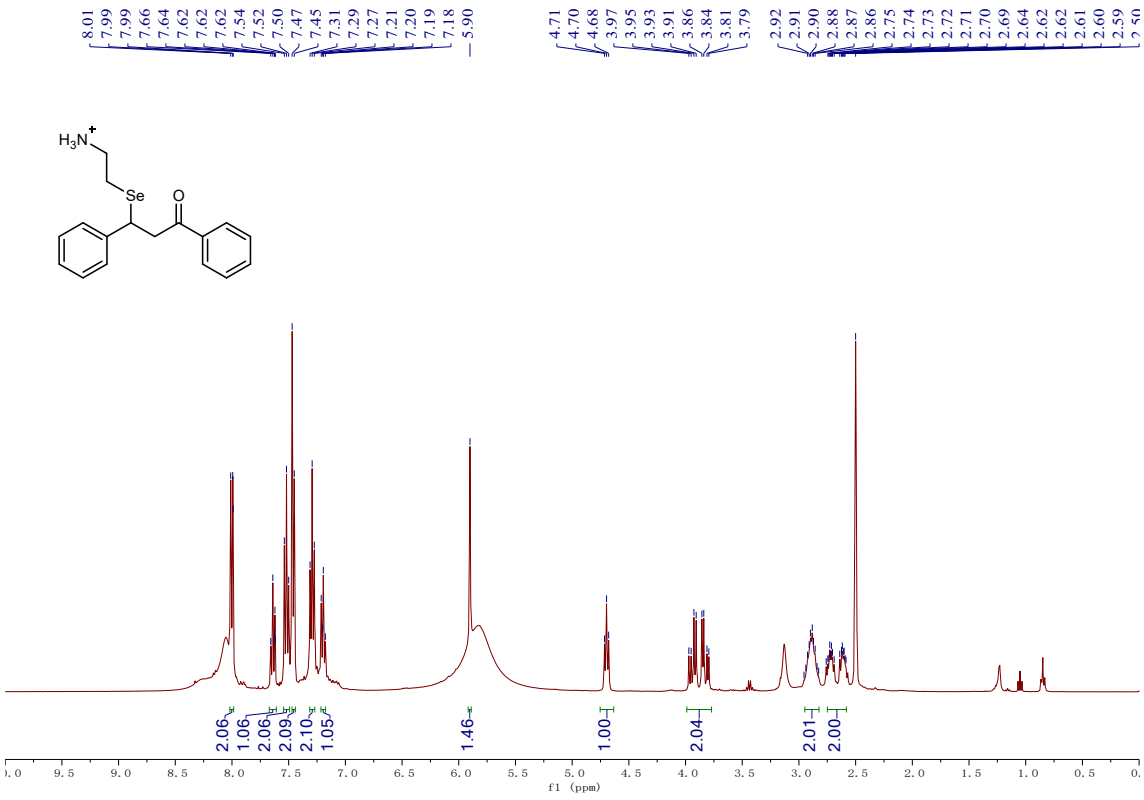

Figure S48. The ^{1}H NMR (400 MHz, DMSO-d_6) spectrum of the solid residues of chalcone substrate obtained after 16-h dark reactions when $DSEACl_2$ is used in stoichiometric amounts.

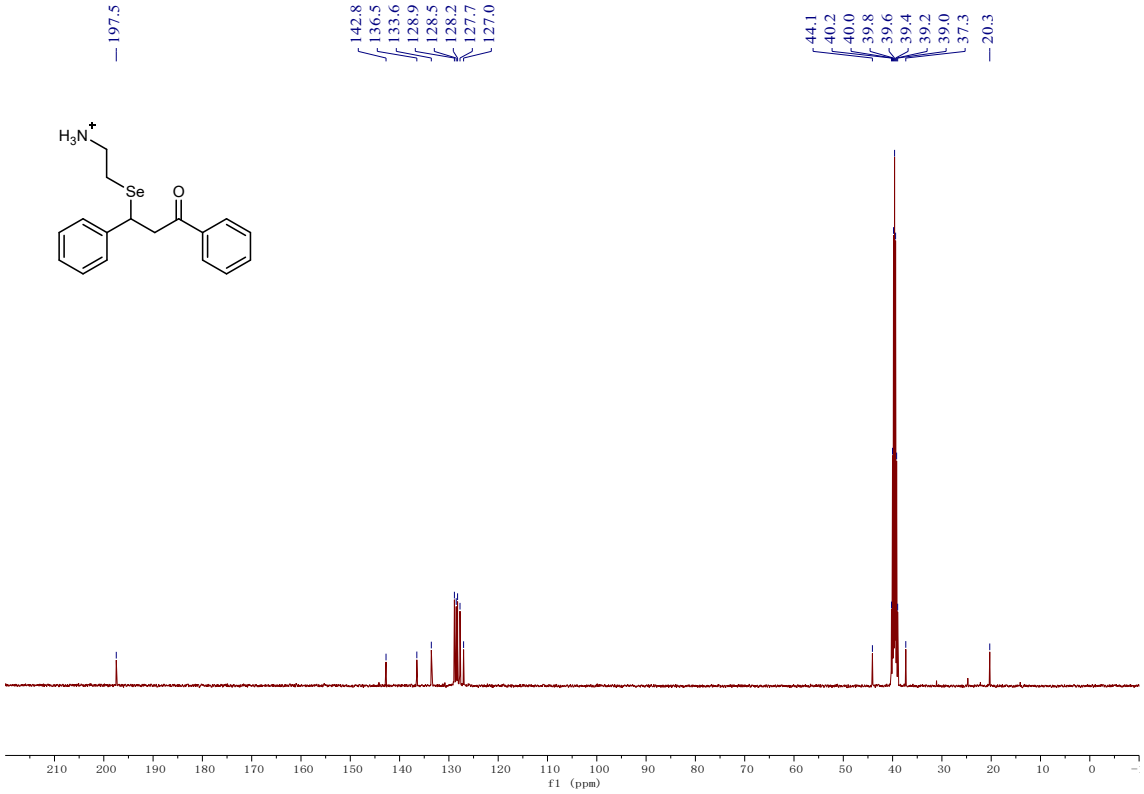

Figure S49. The ^{13}C NMR (101 MHz, DMSO-d_6) spectrum of the solid residues of chalcone substrate obtained after 16-h dark reactions when $DSEACl_2$ is used in stoichiometric amounts.

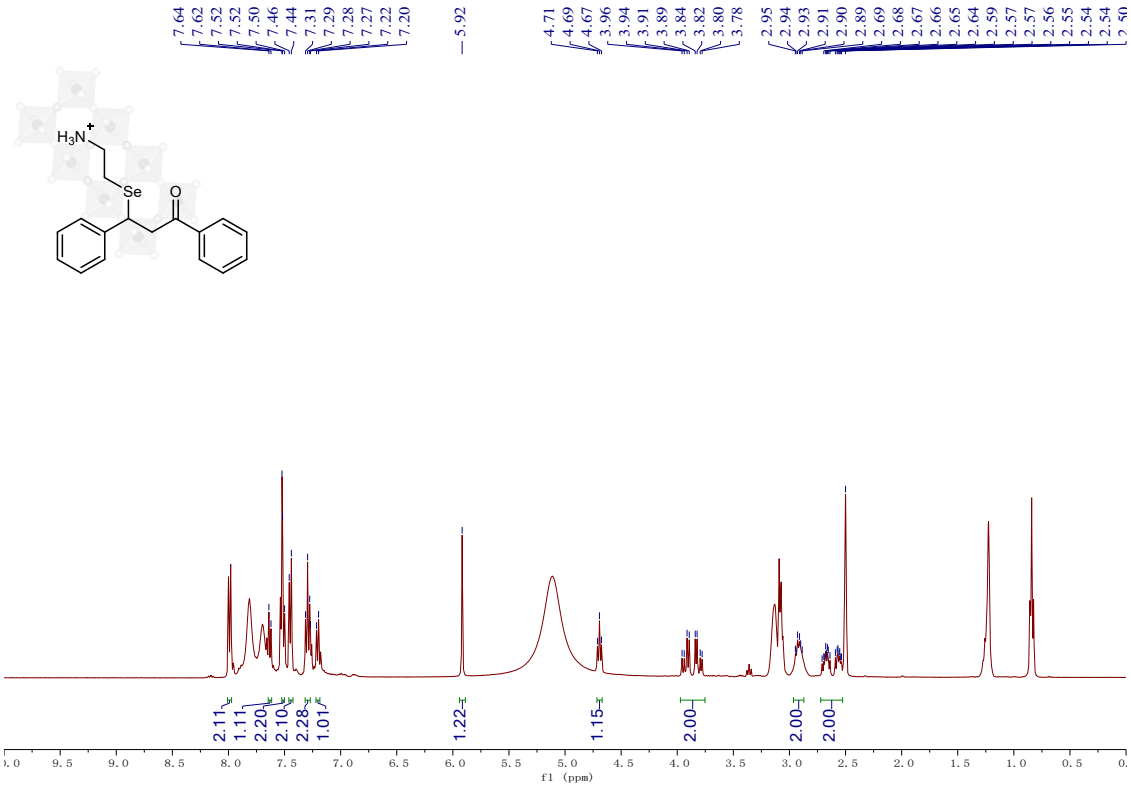

Figure S50. **The ^{1}H NMR (400 MHz, DMSO-d_6) spectrum of the solid residues of chalcone substrate obtained after 16-h dark reactions when $(SEA)_2PbI_4$ is used in stoichiometric amounts.**

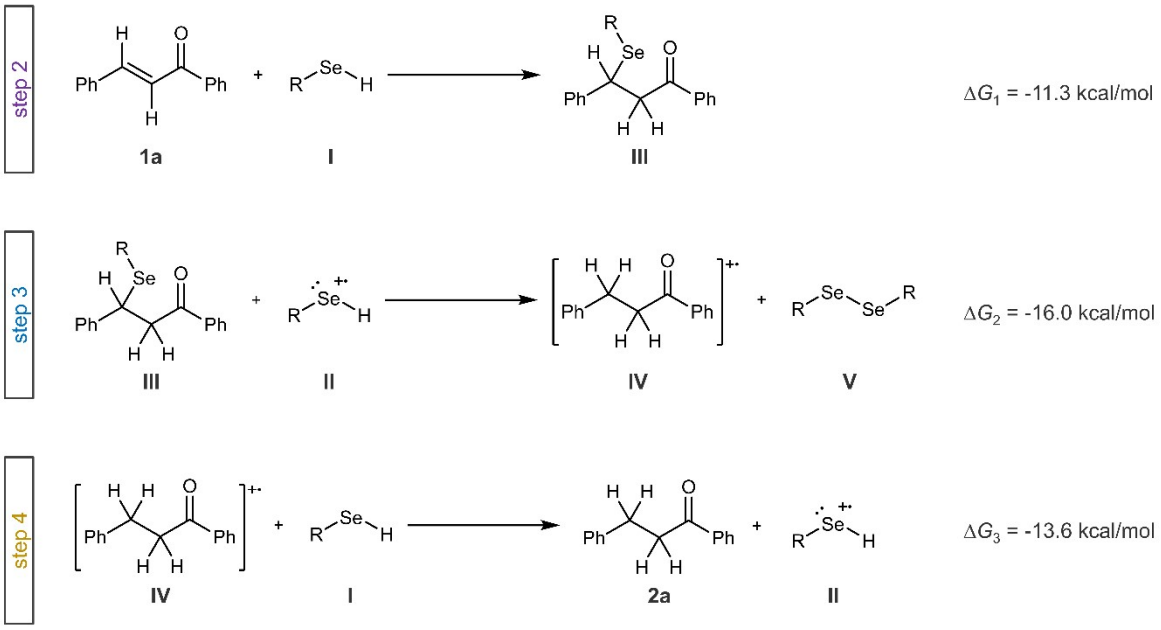

6. Mechanism study

Scheme S1. The corresponding reaction Gibbs free energies for proposed key steps of the surface-selenol-promoted catalytic reaction shown in Figure 4c. The calculation is based on the homogenous reaction between chalcone (i.e., Substrate **1a**) and surface selenol-containing cation RSeH = $NH_3^+CH_2CH_2SeH$. The subscript numbers of each compound are consistent with Figure 4c.

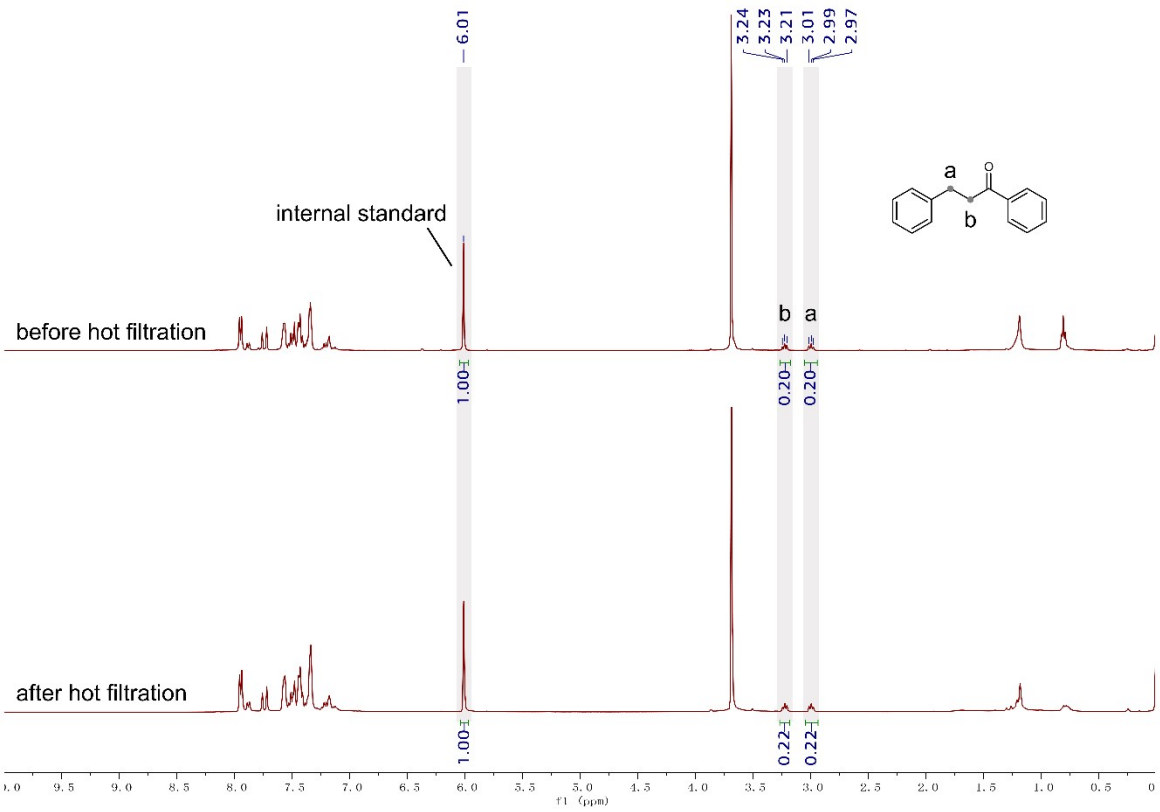

Figure S51. ^{1}H NMR spectra (400 MHz, $CDCl_3$) of the reaction mixture of chalcone 1a before and after the hot filtration test. The reaction was conducted with solid $(SEA)_2PbI_4$ for 4 h, followed by the removal of the catalyst and further irradiation for 12 h under identical conditions. The yields were calculated using 1,3,5-trimethoxybenzene as the internal standard.

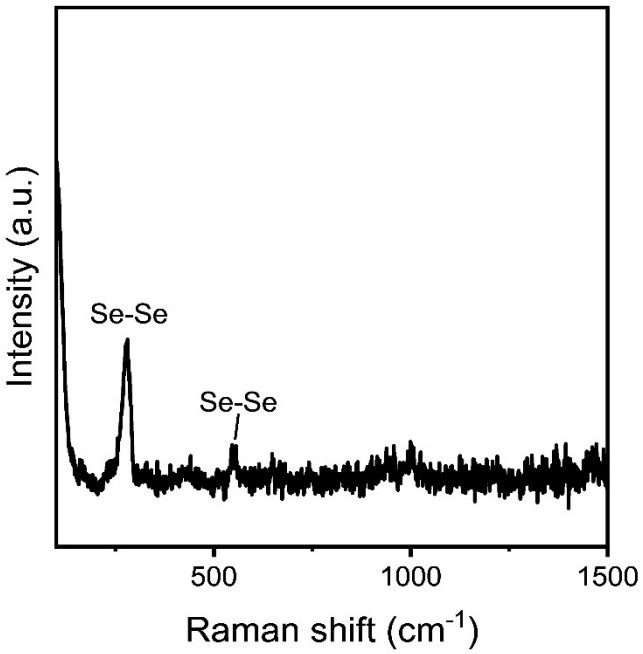

Figure S52. **Raman spectrum of the $(SEA)_2PbI_4$ crystals after repeated redox reaction cycling, which leads to the gradual removal and conversion of SEA moieties into the more stable DSEA species.**

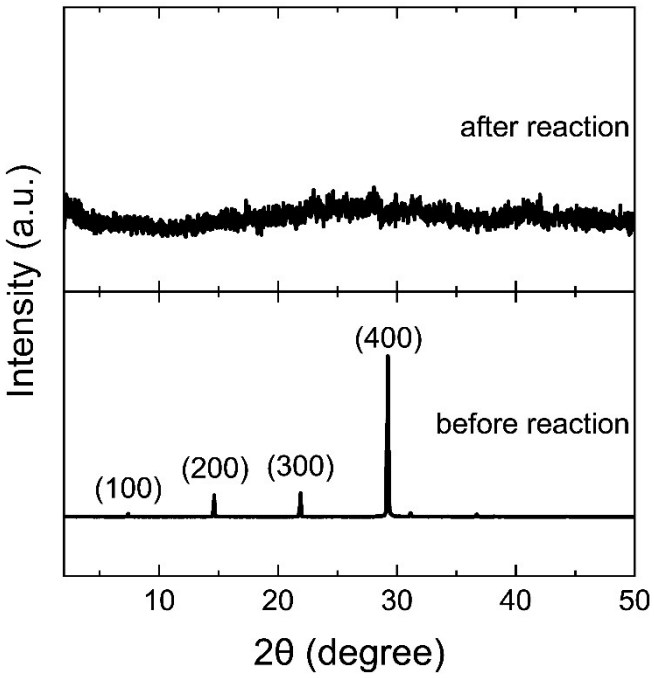

Figure S53. PXRD patterns of $(SEA)_2PbI_4$ crystals before and after photocatalytic reaction.

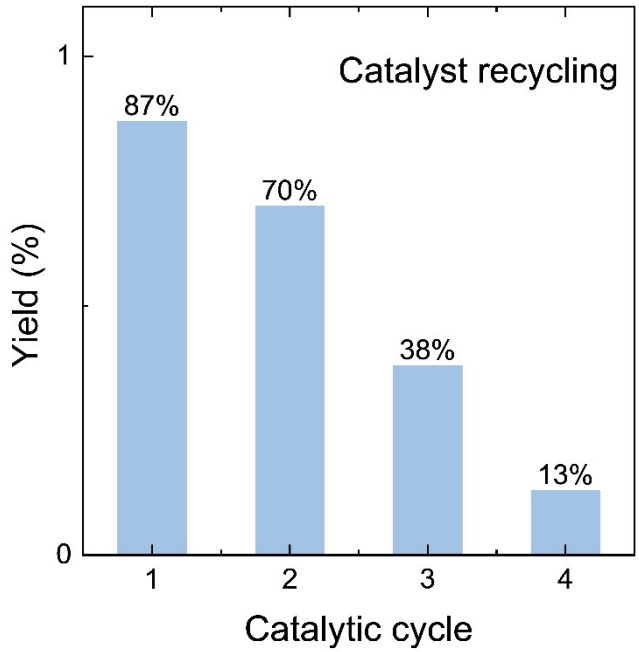

Figure S54. Recyclability of $(SEA)_2PbI_4$ photocatalyst. Product yields for the reduction of chalcone (**1a**) over four consecutive cycles under identical reaction conditions.

7. References

1 G. Kresse and J. Furthmüller, Efficiency of ab-initio total energy calculations for metals and semiconductors using a plane-wave basis set, *Computational Materials Science*, 1996, **6**, 15-50.

2 P. E. Blochl, Projector augmented-wave method, *Phys. Rev. B*, 1994, **50**, 17953-17979.

3 John, P., Perdew, Kieron, Burke, Matthias, Ernzerhof and Erratum, Generalized Gradient Approximation Made Simple, *Phys. Rev. Lett.*, 1996, **77**, 3865-3868.

4 R. Nelson, C. Ertural, J. George, V. Deringer and R. Dronskowski, LOBSTER: Local Orbital Projections, Atomic Charges, and Chemical Bonding Analysis from Projector-Augmented-Wave-Based DFT, *J. Comput. Chem.*, 2020, **41**, 1-10.

5 Izumi and Momma, VESTA 3 for three-dimensional visualization of crystal, volumetric and morphology data, *J. Appl. Cryst.*, 2011, **44**, 1272–1276.

6 N. Mercier, S. Poiroux, A. Riou and P. Batail, Unique Hydrogen Bonding Correlating with a Reduced Band Gap and Phase Transition in the Hybrid Perovskites $(HO(CH_2)_2NH_3)_2PbX_4$ (X = I, Br), *Inorg. Chem.*, 2004, **43**, 8361-8366.

7 Z. Yuan, L. Zhao, E. Pradhan, M. Lai, T. Zeng and Z. Yang, Postsynthetic Crystalline Transformation in Two-Dimensional Perovskites via Organothiol-Based Chemistry, *CCS Chem.*, 2022, **4**, 855-863.

8 J. Zhang, M. Song, W. Tang, D. Xue, J. Xiao, H. Sun and C. Wang, Transforming Racemic Compounds into Two New Enantioenriched Chiral Products via Intermediate Kinetic Resolution, *ACS Catal.*, 2023, **13**, 15603-15610.

9 D. Zhu, L. Lv, C.-C. Li, S. Ung, J. Gao and C.-J. Li, Umpolung of Carbonyl Groups as Alkyl Organometallic Reagent Surrogates for Palladium-Catalyzed Allylic Alkylation, *Angew. Chem. Int. Ed.*, 2018, **57**, 16520-16524.

10 A. A. Golovanov, D. R. Latypova, V. V. Bekin, V. S. Pisareva, A. V. Vologzhanina and V. A. Dokichev, Synthesis of 1,5-disubstituted (E)-pent-2-en-4-yn-1-ones, *Russ. J. Org. Chem.*, 2013, **49**, 1264-1269.

11 Z. Zhang, A. Huang, L. Ma, J. H. Xu and M. Zhang, A facile metal-free one-flask

synthesis of multi-substituted furans via a $BF_3.Et_2O$ mediated formal [4 + 1] reaction of 3-chloro-3-phenyldiazirines and *α*,*β*-alkenyl ketones, *RSC Adv.*, 2022, **12**, 15190-15195.

12 H. Nitta, K. Takimoto and I. Ueda, Synthesis and Structures of 6-Aryl-1,5-dimethoxycarbonyl-2-methyl-4-morpholino-1,3-cyclohexadienes and Related Compounds, *Chem. Pharm. Bull.*, 1992, **40**, 858-863.

13 S. J. Yim, M. H. Kim and D. K. An, Effective Partial Alkynylation of Carboxylic Acid Derivatives to Alkynyl Ketones, *Bull. Korean Chem. Soc.*, 2010, **31**, 286-290.

14 I. Kisets, Z. Sofiya and D. Gelman, Synthesis and Catalytic Properties of a Carbometalated Half-Sandwich Ru(II) Complex Bearing a Rigid Polyaromatic Tether, *Organometallics*, 2022, **41**, 76-82.

15 D. Bhattacharyya, B. K. Sarmah, S. Nandi, H. K. Srivastava and A. Das, Selective Catalytic Synthesis of *α*-Alkylated Ketones and *β*-Disubstituted Ketones via Acceptorless Dehydrogenative Cross-Coupling of Alcohols, *Org. Lett.*, 2021, **23**, 869-875.

16 K. Nicholson, T. Langer and S. P. Thomas, Borane-Catalyzed, Chemoselective Reduction and Hydrofunctionalization of Enones Enabled by B-O Transborylation, *Org. Lett.*, 2021, **23**, 2498-2504.

17 K. Dey and G. de Ruiter, Chemoselective Hydrogenation of *α*,*β*-Unsaturated Ketones Catalyzed by a Manganese(I) Hydride Complex, *Org. Lett.*, 2024, **26**, 4173-4177.

18 H. Wang, L. Chen, Y. Chen and Y. Zhang, Highly efficient iron-catalyzed conjugate reduction of *α*,*β*-unsaturated ketones with polymethylhydrosiloxane, *Org. Biomol. Chem.*, 2024, **22**, 5097-5100.

19 J. Wu, X. Tang, H. Liu, F. Xue and M. Wang, Neutral-Eosin Y-Catalyzed Regioselective Hydroacylation of Aryl Alkenes under Visible-Light Irradiation, *Synlett*, 2021, **32**, 406-410.

20 X. Y. Zhan, H. Zhang, Y. Dong, J. Yang, S. He, Z. C. Shi, L. Tang and J. Y. Wang, Chemoselective Hydrosilylation of the *α*,*β*-Site Double Bond in *α*,*β*- and *α*,*β*,*γ*,*δ*-

Unsaturated Ketones Catalyzed by Macrosteric Borane Promoted by Hexafluoro-2-propanol, *J. Org. Chem.*, 2020, **85**, 6578-6592.

21 B. Q. Cheng, S. X. Zhang, Y. Y. Cui, X. Q. Chu, W. Rao, H. Xu, G. Z. Han and Z. L. Shen, Copper(II)-Mediated Ring Opening/Alkynylation of Tertiary Cyclopropanols by Using Nonmodified Terminal Alkynes, *Org. Lett.*, 2020, **22**, 5456-5461.

22 N. Garg, H. P. Somasundharam, P. Dahiya and B. Sundararaju, Methanol as a hydrogen source: room-temperature highly-selective transfer hydrogenation of *α*,*β*-unsaturated ketones, *Chem. Commun.*, 2022, **58**, 9930-9933.

23 Z. Q. Zhu, J. S. He, H. J. Wang and Z. Z. Huang, Domino Reactions Containing Different Types of Heck Reactions for Selective 3,3- and 1,3-Diarylations of Propenol with Aryl Halides by Triple Catalysis, *J. Org. Chem.*, 2015, **80**, 9354-9359.

24 S. Genç, B. Arslan, D. Gülcemal, S. Gülcemal and S. Günnaz, Nickel-catalyzed alkylation of ketones and nitriles with primary alcohols, *Org. Biomol. Chem.*, 2022, **20**, 9753-9762.

25 M. Kenny, J. Christensen, S. J. Coles and V. Franckevičius, Regioswitchable Palladium-Catalyzed Decarboxylative Coupling of 1,3-Dicarbonyl Compounds, *Org. Lett.*, 2015, **17**, 3926-3929.